RAA 2017 Vol. **17** No. **1**, 5 (16pp) doi: 10.1088/1674–4527/17/1/5

http://www.raa-journal.org *http://iopscience.iop.org/raa*

***R**esearch in*
***A**stronomy and*
***A**strophysics*

Stellar parameters of main sequence turn-off star candidates observed with LAMOST and *Kepler*

Ya-Qian Wu[1], Mao-Sheng Xiang[2], Xian-Fei Zhang[1], Tan-Da Li[2], Shao-Lan Bi[1], Xiao-Wei Liu[3], Jian-Ning Fu[1], Yang Huang[3], Zhi-Jia Tian[3], Kang Liu[1], Zhi-Shuai Ge[1], Xin He[1] and Jing-Hua Zhang[1]

[1] Department of Astronomy, Beijing Normal University, Beijing 100875, China; *wuyaqian@mail.bnu.edu.cn; bisl@bnu.edu.cn*
[2] National Astronomical Observatories, Chinese Academy of Sciences, Beijing 100012, China
[3] Department of Astronomy, Peking University, Beijing 100871, China

Received 2016 July 26; accepted 2016 September 16

Abstract Main sequence turn-off (MSTO) stars have advantages as indicators of Galactic evolution since their ages can be robustly estimated from atmospheric parameters. Hundreds of thousands of MSTO stars have been selected from the LAMOST Galactic survey to study the evolution of the Galaxy, and it is vital to derive accurate stellar parameters. In this work, we select 150 MSTO star candidates from the MSTO star sample of Xiang that have asteroseismic parameters and determine accurate stellar parameters for these stars by combining asteroseismic parameters deduced from *Kepler* photometry and atmospheric parameters deduced from LAMOST spectra. With this sample, we examine the age determination as well as the contamination rate of the MSTO star sample. A comparison of age between this work and Xiang shows a mean difference of 0.53 Gyr (7%) and a dispersion of 2.71 Gyr (28%). The results show that 79 of the candidates are MSTO stars, while the others are contaminations from either main sequence or sub-giant stars. The contamination rate for the oldest stars is much higher than that for younger stars. The main cause for the high contamination rate is found to be the relatively large systematic bias in the LAMOST surface gravity estimates.

Key words: stars: fundamental parameters — stars: evolution — stars: asteroseismology

1 INTRODUCTION

A star begins its evolution as a hydrogen-rich main-sequence star with a hydrogen-burning core. As core hydrogen burning finishes, hydrogen-shell burning starts and the star expands to larger radius, lower surface temperature and higher luminosity, and the star evolves into the sub-giant branch phase. Main sequence turn-off (MSTO) stars are stars that have reached the point of central hydrogen exhaustion at the end of the main-sequence phase. Given the metallicity, their effective temperatures are very sensitive to their ages, hence one can obtain reliable age estimates for MSTO stars given accurate measurements of effective temperatures.

MSTO stars are widely used to determine ages of star clusters as they are easily identified from color-magnitude diagrams (CMDs) (e.g. Mackey et al. 2008; Goudfrooij et al. 2009; Yang et al. 2013). Since member stars of a cluster are generally believed to form from the same gas cloud simultaneously, they have the same age. Unlike MSTO stars in clusters, MSTO stars in the field are not easy to identify from CMDs. To identify field MSTO stars, accurate estimates of atmospheric parameters ($T_{\rm eff}$, $\log g$ and [Fe/H]) are required. From results provided by the LAMOST Experiment for Galactic Understanding and Exploration (LEGUE; Deng et al. 2012; Zhao et al. 2012; Liu et al. 2014) and other spectroscopic surveys such as the Sloan Extension for Galactic Understanding and Exploration (SDSS/SEGUE; Yanny et al. 2009), the Radial Velocity Experiment (RAVE; Steinmetz et al. 2006) and the Apache Point Observatory

Galactic Evolution Experiment (APOGEE; Majewski et al. 2010), stellar atmospheric parameters of millions of stars are available from survey spectra. Typical accuracies of LAMOST stellar atmospheric parameters reach 100 – 150 K for $T_{\rm eff}$, 0.20 – 0.25 dex for $\log g$ and 0.1 – 0.2 dex for [Fe/H] (Xiang et al. 2015a; Wu et al. 2014; Luo et al. 2015,). Hundreds of thousands of MSTO stars have been selected from the LAMOST survey by Xiang et al. (2015b) based on stellar atmospheric parameters yielded by the LAMOST Stellar Parameter Pipeline at Peking University (LSP3; Xiang et al. 2015a). The ages of these MSTO stars are also estimated, with a claimed uncertainty of about 30 per cent. However, given the low spectral resolution of LAMOST ($R\sim$1800; e.g. Cui et al. 2012; Deng et al. 2012), accurate stellar parameters, especially surface gravity, are difficult to obtain from the spectra. Therefore, a careful sanity check on the feasibility of the method to select the MSTO star sample and on the accuracy of age estimation seems to be essential.

Asteroseismology is a powerful tool to derive accurate stellar parameters (Bi et al. 2008; Gilliland et al. 2010; Yang & Meng 2010; Chaplin et al. 2011; Stello et al. 2013; Tian et al. 2015). By asteroseismology, accurate stellar parameters of thousands of stars have been obtained (Chaplin et al. 2014; Huber et al. 2014). It is found that surface gravities yielded by asteroseismology can be accurate to 0.01 – 0.03 dex (Hekker et al. 2013; Huber et al. 2014), much better than the spectroscopic estimates. Combining effective temperatures and metallicities from LAMOST spectra with asteroseismic surface gravity yielded from *Kepler* photometry, MSTO stars can be clearly identified and their ages can also be accurately determined.

In this paper, we determine fundamental stellar parameters (M, R, Age, L, $T_{\rm eff}$, Z, $\log g$) for 150 MSTO star candidates selected from the MSTO star sample that have asteroseismic properties available from photometry of the *Kepler* mission (Gilliland et al. 2010). Meanwhile, we compare our results with previous studies by Huber et al. (2014) and Xiang et al. (2015b). We discuss the impact of uncertainties in atmospheric parameters on the measurement of ages, and examine the accuracy of the age estimates as well as the contamination rate of the MSTO star sample. The paper is organized as follows. In Section 2, we introduce how to select the sample of MSTO star candidates. In Section 3, we describe the stellar model and how to obtain the stellar parameters. Results and discussion are presented in Section 4 and a summary is provided in Section 5.

2 THE MSTO STAR CANDIDATES

The LAMOST-*Kepler* project (De Cat et al. 2015) aims to observe stars in the *Kepler* field with LAMOST (Cui et al. 2012) and deliver atmospheric parameters and radial velocities. The LAMOST survey (Zhao et al. 2012) has produced a large number of low resolution ($R\sim$1800) optical spectra (λ 3800 – 9000 Å). By September 2014, all the *Kepler* fields had been observed at least once, and 101 086 spectra had been collected on 38 LAMOST plates (De Cat et al. 2015). Many of the stars have asteroseismic characteristics deduced from *Kepler* photometry. These stars have been used to examine and calibrate stellar surface gravities yielded from the LAMOST spectra (Ren et al. 2016; Wang et al. 2016).

To study the evolution of the Galaxy, Xiang et al. (2015b) have selected a sample of 0.3 million MSTO stars from the LAMOST survey based on stellar atmospheric parameters ($T_{\rm eff}$, $\log g$ and [Fe/H]) derived by the LSP3. They have estimated stellar ages for those MSTO stars with an isochrone fitting technique utilizing the Yonsei-Yale (YY) isochrones (Demarque et al. 2004), and claim a typical accuracy of 30 per cent.

Among the LAMOST-*Kepler* stars, about 4000 stars are found to have asteroseismic parameters, which are the frequency of maximum power of the oscillation $\nu_{\rm max}$ and large frequency spacing $\Delta\nu$, from literature (Hekker et al. 2011; Appourchaux et al. 2012; Mosser et al. 2012; Stello et al. 2013; Huber et al. 2013; Chaplin et al. 2014), most of which are red giant stars and only about 300 stars are dwarfs/subgiants. A cross-identification with the MSTO star sample yields 179 common stars, and in this work, we denote them as MSTO star candidates. Asteroseismic parameters collected from the literature, as well as atmospheric parameters yielded by the LSP3 for these MSTO star candidates, are listed in Table 1.

3 GRID MODELING

3.1 Models

We use the Yale Rotating Stellar Evolution Code (YREC; Pinsonneault et al. 1990, 1992; Demarque et al. 2008) to construct stellar evolution models. Input physics include the OPAL equation of state tables (Rogers & Nayfonov 2002) and OPAL high-temperature opacities (Iglesias & Rogers 1996) supplemented with low-temperature opacities of Ferguson et al. (2005). The NACRE nuclear reaction rates (Bahcall et al. 1995) are used. Atomic diffusion due to concentration and thermal gradients is included in the computation of models with initial masses below

Table 1 Spectroscopic and Asteroseismic Parameters of 179 Targets

Star KIC	$T_{\rm eff}$ (K)	$\log g$ (dex)	[Fe/H] (dex)	$\Delta\nu$ (μHz)	$\nu_{\rm max}$ (μHz)	Ref.
1725815	6195 ± 151	4.08 ± 0.23	0.04 ± 0.11	55.4 ± 1.3	1045 ± 47	[1]
2010607	6113 ± 100	4.09 ± 0.21	0.16 ± 0.09	42.5 ± 1.7	675 ± 86	[1]
2865774	5792 ± 93	4.13 ± 0.20	0.07 ± 0.09	62.7 ± 2.7	1252 ± 90	[1]
2998253	6116 ± 100	4.19 ± 0.19	0.16 ± 0.09	89.0 ± 3.6		[1]
3112152	5967 ± 97	4.10 ± 0.20	-0.03 ± 0.09	63.9 ± 1.9	1219 ± 67	[1]
3123191	6145 ± 101	4.19 ± 0.19	-0.05 ± 0.10	89.8 ± 2.2		[1]
3241581	5577 ± 89	4.21 ± 0.18	0.27 ± 0.09	122.9 ± 1.6		[1]
3344897	6240 ± 104	4.18 ± 0.20	0.07 ± 0.10	46.5 ± 0.8	874 ± 56	[1]
3438633	6082 ± 100	4.12 ± 0.20	-0.17 ± 0.10	55.8 ± 1.7	987 ± 56	[1]
3456181	6236 ± 104	4.17 ± 0.20	0.07 ± 0.10	52.0 ± 0.8	921 ± 30	[1]
3656476	5568 ± 89	4.14 ± 0.19	0.30 ± 0.09	93.3 ± 1.3	1887 ± 40	[1]
3942719	5659 ± 90	4.16 ± 0.19	-0.31 ± 0.11	45.9 ± 3.7	780 ± 38	[1]
3967859	5888 ± 95	4.15 ± 0.20	-0.27 ± 0.10	93.6 ± 3.0		[1]
4049576	5803 ± 93	4.09 ± 0.20	-0.19 ± 0.10	51.9 ± 1.7	942 ± 70	[1]
4141376	5903 ± 95	4.10 ± 0.20	-0.28 ± 0.11	128.8 ± 1.3	2928 ± 97	[2]
4143755	5681 ± 91	4.10 ± 0.20	-0.50 ± 0.14	77.2 ± 1.3	1458 ± 57	[2]
4165030	5675 ± 91	4.30 ± 0.17	-0.29 ± 0.10	61.8 ± 1.5	1102 ± 52	[1]
4252818	5680 ± 91	4.30 ± 0.17	0.08 ± 0.09	69.2 ± 7.4	1318 ± 65	[1]
4349452	6161 ± 102	4.16 ± 0.20	-0.00 ± 0.09	98.27 ± 0.57	2106 ± 50	[2]
4465324	5767 ± 111	4.21 ± 0.19	0.03 ± 0.10	86.2 ± 2.8	1744 ± 64	[1]
4543171	5886 ± 114	4.23 ± 0.19	0.16 ± 0.10	71.0 ± 1.7	1480 ± 54	[1]
4554830	5509 ± 86	4.18 ± 0.18	0.32 ± 0.09	85.6 ± 1.2	1751 ± 42	[1]
4577484	5588 ± 90	4.23 ± 0.18	0.22 ± 0.09	47.0 ± 1.4	817 ± 63	[1]
4646780	6344 ± 108	4.11 ± 0.21	-0.14 ± 0.10	59.3 ± 1.8	1104 ± 76	[1]
4672403	5774 ± 92	4.04 ± 0.21	0.23 ± 0.09	60.3 ± 1.2	1107 ± 44	[1]
4739932	5847 ± 94	4.21 ± 0.19	0.18 ± 0.09	60.9 ± 1.4	1132 ± 78	[1]
4755204	5913 ± 95	4.24 ± 0.19	0.07 ± 0.09	70.4 ± 1.2	1360 ± 42	[1]
4841753	5976 ± 97	4.14 ± 0.20	0.19 ± 0.09	50.2 ± 1.9	871 ± 103	[1]
4842436	5761 ± 92	4.26 ± 0.18	0.24 ± 0.09	72.6 ± 3.0	1339 ± 115	[1]
4914423	5852 ± 94	4.23 ± 0.18	0.15 ± 0.09	81.5 ± 1.6	1663 ± 56	[2]
4914923	5766 ± 92	4.20 ± 0.19	0.21 ± 0.09	88.6 ± 0.3	1849 ± 46	[1]
4947253	5909 ± 95	4.12 ± 0.20	-0.02 ± 0.09	52.6 ± 1.0	923 ± 40	[1]
5088536	5830 ± 93	4.23 ± 0.18	-0.11 ± 0.09	109.6 ± 3.1		[2]
5094751	5826 ± 93	4.24 ± 0.19	0.01 ± 0.09	91.1 ± 2.3	1745 ± 117	[2]
5095159	5305 ± 87	4.24 ± 0.17	0.18 ± 0.09	35.0 ± 0.5	582 ± 29	[1]
5095850	6622 ± 118	4.00 ± 0.23	0.15 ± 0.11	46.7 ± 3.2	791 ± 37	[1]
5253542	5685 ± 114	4.22 ± 0.19	0.25 ± 0.10	108.4 ± 1.8		[1]
5353186	6038 ± 98	4.12 ± 0.20	0.17 ± 0.09	47.4 ± 1.2	872 ± 31	[1]
5511081	5826 ± 93	4.25 ± 0.18	0.02 ± 0.09	63.3 ± 3.4		[2]
5512589	5720 ± 91	4.15 ± 0.19	0.20 ± 0.09	68.2 ± 0.7	1224 ± 43	[1]
5523099	5513 ± 89	4.24 ± 0.18	0.03 ± 0.09	41.8 ± 0.9	722 ± 31	[1]
5561278	5984 ± 97	4.00 ± 0.15	-0.03 ± 0.09	56.2 ± 1.7	1023 ± 36	[2]
5636956	6214 ± 103	4.10 ± 0.21	0.21 ± 0.10	55.4 ± 0.9	1007 ± 36	[1]
5686856	5897 ± 95	4.16 ± 0.19	0.11 ± 0.09	62.3 ± 1.7	1081 ± 29	[1]
5689219	6278 ± 105	4.16 ± 0.20	-0.24 ± 0.11	64.8 ± 1.0	1282 ± 76	[1]
5780885	5969 ± 97	4.08 ± 0.21	0.19 ± 0.09	56.4 ± 1.7		[2]
5961597	6300 ± 106	4.09 ± 0.21	0.14 ± 0.10	59.8 ± 0.9	1258 ± 43	[1]
6064910	6172 ± 102	4.03 ± 0.22	-0.21 ± 0.10	43.9 ± 0.8	721 ± 43	[1]
6196457	5877 ± 94	4.12 ± 0.20	0.19 ± 0.09	66.6 ± 1.1	1299 ± 53	[2]
6268648	6032 ± 98	4.09 ± 0.21	-0.25 ± 0.10	88.9 ± 2.0		[2]
6308642	5671 ± 91	4.17 ± 0.19	-0.13 ± 0.09	42.5 ± 0.7	733 ± 28	[1]
6520835	6029 ± 98	4.02 ± 0.22	-0.01 ± 0.09	49.7 ± 0.8	890 ± 32	[1]
6521045	5806 ± 93	4.06 ± 0.21	0.12 ± 0.09	77.0 ± 1.1	1502 ± 31	[2]
6587236	5921 ± 95	4.08 ± 0.21	-0.23 ± 0.10	32.1 ± 1.9	481 ± 25	[1]
6592305	6001 ± 97	4.13 ± 0.20	0.14 ± 0.09	46.8 ± 0.6	842 ± 23	[1]
6593461	5658 ± 90	4.23 ± 0.18	0.23 ± 0.09	90.8 ± 2.0	1927 ± 338	[1]
6603624	5515 ± 89	4.11 ± 0.19	0.29 ± 0.09	110.4 ± 1.7	2402 ± 51	[1]
6605673	6007 ± 98	4.02 ± 0.22	-0.26 ± 0.11	68.0 ± 0.9	1273 ± 49	[1]
6688822	5559 ± 89	4.05 ± 0.20	0.29 ± 0.09	47.1 ± 1.0	811 ± 33	[1]

Table 1 *Continued.*

Star KIC	$T_{\rm eff}$ (K)	$\log g$ (dex)	[Fe/H] (dex)	$\Delta\nu$ (μHz)	$\nu_{\rm max}$ (μHz)	Ref.
6689943	5942 ± 96	4.14 ± 0.20	0.10 ± 0.09	80.7 ± 1.5	1682 ± 66	[1]
6693861	5749 ± 92	4.18 ± 0.19	-0.28 ± 0.10	46.7 ± 1.0	765 ± 42	[1]
6766513	6154 ± 102	4.17 ± 0.20	-0.06 ± 0.10	51.3 ± 1.1	883 ± 84	[1]
6853020	6161 ± 102	4.02 ± 0.22	0.15 ± 0.10	54.8 ± 1.3		[1]
6863041	5622 ± 90	4.06 ± 0.20	0.24 ± 0.09	41.9 ± 1.1	775 ± 32	[1]
7038145	5896 ± 115	4.02 ± 0.22	0.06 ± 0.10	43.0 ± 0.7	764 ± 30	[1]
7107778	5149 ± 87	4.07 ± 0.19	0.11 ± 0.10	31.4 ± 0.6	529 ± 15	[1]
7133688	6291 ± 106	4.08 ± 0.21	0.17 ± 0.10	59.7 ± 2.1	1146 ± 74	[1]
7199397	5915 ± 95	4.02 ± 0.21	-0.07 ± 0.09	38.6 ± 0.68	643 ± 17	[2]
7264595	5665 ± 91	4.01 ± 0.21	-0.12 ± 0.09	36.3 ± 1.6	543 ± 24	[1]
7282890	6266 ± 105	4.13 ± 0.20	0.22 ± 0.10	46.0 ± 0.7	834 ± 49	[1]
7383120	5995 ± 97	4.20 ± 0.19	-0.08 ± 0.09	85.6 ± 2.5	1794 ± 85	[1]
7386523	5840 ± 94	4.11 ± 0.20	0.15 ± 0.09	48.3 ± 2.0	919 ± 113	[1]
7429287	5618 ± 90	4.22 ± 0.19	-0.31 ± 0.11	71.2 ± 1.4	1345 ± 34	[1]
7591963	5903 ± 95	4.19 ± 0.19	0.13 ± 0.09	59.2 ± 0.9	1096 ± 48	[1]
7680114	5810 ± 93	4.23 ± 0.18	0.18 ± 0.09	85.1 ± 1.3	1684 ± 47	[1]
7833440	6051 ± 99	4.13 ± 0.20	-0.27 ± 0.11	66.2 ± 1.1	1118 ± 80	[1]
7880676	6019 ± 98	4.14 ± 0.20	0.11 ± 0.09	53.7 ± 1.0	1017 ± 43	[1]
7910848	5964 ± 96	4.23 ± 0.19	0.16 ± 0.09	73.3 ± 1.4		[1]
8012842	5712 ± 91	4.26 ± 0.18	0.22 ± 0.09	95.8 ± 2.3	2000 ± 251	[1]
8016496	6009 ± 98	3.97 ± 0.22	-0.03 ± 0.09	55.0 ± 1.2	1053 ± 48	[1]
8019508	5994 ± 97	4.08 ± 0.21	0.14 ± 0.09	37.7 ± 2.0	658 ± 35	[1]
8045442	5899 ± 95	4.08 ± 0.21	0.15 ± 0.09	31.8 ± 0.6		[1]
8298626	5969 ± 97	4.13 ± 0.20	-0.02 ± 0.09	91.4 ± 1.6	1861 ± 69	[1]
8349582	5600 ± 90	4.10 ± 0.20	0.24 ± 0.09	83.6 ± 1.4	1677 ± 90	[2]
8367710	6117 ± 140	4.12 ± 0.22	0.07 ± 0.11	56.1 ± 1.1	1085 ± 52	[1]
8391021	6094 ± 100	4.06 ± 0.21	-0.29 ± 0.11	79.7 ± 1.4	1595 ± 45	[1]
8394589	6011 ± 98	4.11 ± 0.20	-0.28 ± 0.11	109.5 ± 1.9	2165 ± 124	[1]
8420801	6155 ± 102	4.17 ± 0.20	0.13 ± 0.10	67.4 ± 1.8	1287 ± 86	[1]
8491374	6197 ± 103	4.17 ± 0.20	0.09 ± 0.10	57.5 ± 2.2	1022 ± 94	[1]
8493735	5884 ± 95	4.02 ± 0.21	-0.02 ± 0.09	38.86 ± 1.94	586.1 ± 29.3	[3]
8493800	5921 ± 95	4.15 ± 0.20	-0.00 ± 0.09	83.6 ± 1.8	1850 ± 109	[1]
8494142	5955 ± 96	4.03 ± 0.22	-0.04 ± 0.09	61.8 ± 0.76	1133 ± 81	[2]
8554498	5866 ± 94	4.21 ± 0.19	0.19 ± 0.09	61.98 ± 0.96	1153 ± 76	[2]
8621637	5679 ± 91	4.22 ± 0.18	0.18 ± 0.09	57.1 ± 1.4	1032 ± 47	[1]
8684730	5915 ± 95	4.13 ± 0.20	0.15 ± 0.09	51.7 ± 1.9	962 ± 39	[2]
8776961	5816 ± 93	4.21 ± 0.09	0.08 ± 0.09	64.7 ± 1.3	1208 ± 33	[1]
8802782	5864 ± 94	3.97 ± 0.22	0.24 ± 0.09	44.9 ± 1.7	784 ± 54	[1]
8817551	5763 ± 92	4.02 ± 0.21	0.25 ± 0.09	42.7 ± 0.8	740 ± 34	[1]
8868481	5591 ± 90	4.12 ± 0.20	0.04 ± 0.09	40.4 ± 1.3	673 ± 42	[1]
8915084	5814 ± 93	4.06 ± 0.21	0.13 ± 0.09	79.1 ± 1.4	1594 ± 59	[1]
8938364	5639 ± 90	4.31 ± 0.17	-0.14 ± 0.09	85.8 ± 1.1	1681 ± 37	[1]
8956017	6221 ± 104	4.00 ± 0.22	0.15 ± 0.10	62.2 ± 2.2	1234 ± 51	[1]
8981766	6190 ± 103	4.14 ± 0.20	0.19 ± 0.10	63.1 ± 1.6	1277 ± 32	[1]
9005973	5821 ± 93	4.28 ± 0.18	0.00 ± 0.09	82.6 ± 2	1560 ± 141	[1]
9116461	6222 ± 104	4.17 ± 0.20	0.03 ± 0.10	104.7 ± 2.3	2334 ± 197	[1]
9335972	5719 ± 91	4.02 ± 0.21	0.13 ± 0.09	46.2 ± 1.6	802 ± 20	[1]
9446628	6146 ± 101	4.17 ± 0.20	-0.04 ± 0.09	56.1 ± 2.5	1031 ± 76	[1]
9451706	5944 ± 96	4.15 ± 0.20	0.22 ± 0.09	95.0 ± 1.6	1988 ± 86	[2]
9451741	5666 ± 91	4.20 ± 0.19	0.22 ± 0.09	94.4 ± 1.9	2079 ± 105	[1]
9592705	6049 ± 99	4.14 ± 0.20	0.17 ± 0.09	53.5 ± 0.32	1008 ± 21	[2]
9664694	6160 ± 102	4.17 ± 0.20	-0.01 ± 0.09	41.2 ± 1.1	722 ± 27	[1]
9696358	5987 ± 97	4.04 ± 0.21	0.12 ± 0.09	51.4 ± 3.7		[2]
9697131	6143 ± 101	4.11 ± 0.21	0.04 ± 0.09	60.2 ± 1.2	1196 ± 80	[1]
9700430	5883 ± 95	4.24 ± 0.18	0.13 ± 0.09	78.9 ± 1.5	1623 ± 94	[1]
9715099	6133 ± 101	4.07 ± 0.21	0.15 ± 0.09	40.7 ± 0.7		[1]
9754284	5941 ± 96	4.19 ± 0.19	0.09 ± 0.09	73.8 ± 1.5	1496 ± 90	[1]
9757640	5505 ± 89	4.17 ± 0.19	0.30 ± 0.09	61.7 ± 1.0	1142 ± 86	[1]
9778067	5899 ± 95	4.13 ± 0.20	-0.45 ± 0.13	50.0 ± 1.7	890 ± 46	[1]
9787965	6064 ± 99	4.16 ± 0.20	0.09 ± 0.09	53.4 ± 2.3	912 ± 60	[1]
9791157	5845 ± 94	4.17 ± 0.19	0.12 ± 0.09	54.4 ± 1.0	984 ± 43	[1]

Table 1 *Continued.*

Star KIC	$T_{\rm eff}$ (K)	$\log g$ (dex)	[Fe/H] (dex)	$\Delta\nu$ (μHz)	$\nu_{\rm max}$ (μHz)	Ref.
9872292	6148 ± 101	4.17 ± 0.20	-0.01 ± 0.09	63.8 ± 1.2		[2]
9962623	5684 ± 91	4.19 ± 0.19	-0.00 ± 0.09	82.2 ± 2.5	1543 ± 164	[1]
10019747	5572 ± 89	4.15 ± 0.19	0.28 ± 0.09	66.7 ± 1.5	1248 ± 41	[1]
10079226	5849 ± 94	4.24 ± 0.18	0.18 ± 0.09	116.4 ± 1.9	2689 ± 93	[1]
10322381	6056 ± 99	4.21 ± 0.19	-0.26 ± 0.11	86.6 ± 4.3	1657 ± 155	[1]
10351059	6247 ± 104	4.09 ± 0.21	0.23 ± 0.10	65.0 ± 0.9	1329 ± 68	[1]
10398597	6153 ± 102	4.10 ± 0.21	0.19 ± 0.10	57.6 ± 1.5	973 ± 85	[1]
10417911	5556 ± 89	4.06 ± 0.20	0.29 ± 0.09	56.1 ± 2.8	1022 ± 61	[1]
10586004	5766 ± 92	4.19 ± 0.19	0.25 ± 0.09	69.2 ± 1.4	1395 ± 40	[2]
10727922	5997 ± 97	4.11 ± 0.20	-0.15 ± 0.10	55.4 ± 2.9	979 ± 56	[1]
10731424	6158 ± 102	4.02 ± 0.22	0.03 ± 0.09	37.6 ± 2.3	670 ± 45	[1]
10732098	5766 ± 92	4.19 ± 0.19	0.13 ± 0.09	62.1 ± 1.1	1082 ± 37	[1]
10875245	5707 ± 91	4.22 ± 0.18	0.25 ± 0.09	86.7 ± 3.7	1711 ± 107	[2]
10923629	6013 ± 98	4.05 ± 0.21	0.20 ± 0.09	42.5 ± 0.8	711 ± 37	[1]
11083308	6021 ± 98	4.20 ± 0.19	0.07 ± 0.09	51.2 ± 1.3	902 ± 39	[1]
11133306	5910 ± 95	4.23 ± 0.18	0.00 ± 0.09	107.9 ± 1.9	2381 ± 95	[2]
11138101	6152 ± 102	4.10 ± 0.21	0.05 ± 0.09	43.8 ± 1.3		[1]
11188219	5793 ± 93	4.26 ± 0.18	0.24 ± 0.09	95.6 ± 3.4	1843 ± 106	[1]
11193681	5597 ± 90	4.05 ± 0.20	0.26 ± 0.09	42.1 ± 0.7	749 ± 36	[1]
11244118	5600 ± 90	4.11 ± 0.20	0.26 ± 0.09	71.3 ± 0.9	1420 ± 31	[1]
11506988	6220 ± 104	4.21 ± 0.19	-0.16 ± 0.10	58.7 ± 1.0	1056 ± 81	[1]
11507653	5847 ± 94	4.17 ± 0.19	0.22 ± 0.09	70.0 ± 2.3	1359 ± 217	[1]
11611414	6033 ± 98	4.20 ± 0.19	-0.02 ± 0.09	68.3 ± 3.3	1162 ± 127	[1]
11771760	5859 ± 94	4.09 ± 0.20	0.04 ± 0.09	32.4 ± 0.7	535 ± 19	[1]
11817562	5970 ± 97	4.01 ± 0.22	0.20 ± 0.09	41.1 ± 0.7	713 ± 46	[1]
11919192	6358 ± 108	4.02 ± 0.22	-0.16 ± 0.11	46.8 ± 1.7	903 ± 48	[1]
11971746	5861 ± 94	4.22 ± 0.19	0.25 ± 0.09	90.8 ± 2.1	1911 ± 124	[1]
12068975	5958 ± 96	4.17 ± 0.19	-0.31 ± 0.11	108.4 ± 3.1	2298 ± 105	[2]
12069127	6223 ± 104	4.13 ± 0.20	0.18 ± 0.10	48.2 ± 0.9	829 ± 41	[1]
12265063	5944 ± 96	4.22 ± 0.19	-0.05 ± 0.09	67.9 ± 1.5	1314 ± 139	[1]
4167879	5770 ± 109	4.14 ± 0.20	-0.24 ± 0.11	3.22 ± 0.059	34.48 ± 5.64	[6]
4245297	5763 ± 92	4.22 ± 0.18	0.16 ± 0.09	3.42 ± 0.078	32.50 ± 3.35	[6]
4466582	5627 ± 90	4.30 ± 0.17	0.09 ± 0.09	10.334 ± 1.033	116.809 ± 11.68	[5]
4581415	5827 ± 103	4.01 ± 0.22	-0.32 ± 0.12	3.5325 ± 0.086	30.454 ± 2.157	[6]
5176520	5444 ± 88	4.36 ± 0.16	-0.50 ± 0.14	12.81 ± 1.281	153.731 ± 15.37	[5]
5649546	5744 ± 107	4.06 ± 0.21	0.11 ± 0.10			
5683538	5860 ± 94	4.09 ± 0.20	-0.52 ± 0.14	42 ± 1.4	695 ± 32	[1]
5814204	6288 ± 106	4.12 ± 0.20	0.03 ± 0.10	5.02 ± 0.12	51.924 ± 2.37	[6]
5892169	5730 ± 88	4.08 ± 0.20	0.08 ± 0.09	29.9 ± 0.4	492 ± 16	[1]
6209592	5946 ± 145	3.99 ± 0.26	-0.40 ± 0.16			
6290627	5352 ± 87	4.06 ± 0.20	-0.20 ± 0.10	22.4 ± 2.24	318.4 ± 31.84	[3]
6347797	6664 ± 136	4.15 ± 0.20	-0.24 ± 0.13			
6363365	5894 ± 95	4.20 ± 0.19	-0.64 ± 0.18	86.3 ± 1.4	1629 ± 80	[1]
6763633	6321 ± 107	4.11 ± 0.21	0.20 ± 0.10			
6852624	5700 ± 92	4.23 ± 0.18	-0.30 ± 0.11			
7955597	5780 ± 92	4.15 ± 0.19	0.11 ± 0.09	12.46 ± 0.23	155.63 ± 7.33	[6]
8520552	7383 ± 154	4.02 ± 0.22	-0.57 ± 0.22	6.2147 ± 0.172	60.498 ± 1.439	[6]
8747199	5664 ± 122	4.25 ± 0.19	-0.60 ± 0.21			
9697262	5409 ± 88	4.06 ± 0.20	-0.08 ± 0.09			
9723621	5795 ± 93	4.10 ± 0.20	0.19 ± 0.09	6.04 ± 0.13	67.96 ± 4.41	[6]
9768011	7322 ± 210	3.96 ± 0.25	-0.80 ± 0.35	57 ± 3.2	918 ± 48	[1]
9778260	5543 ± 89	4.24 ± 0.18	0.01 ± 0.09			
9906321	5604 ± 90	4.13 ± 0.19	-0.17 ± 0.10	5.24 ± 0.15	49.76 ± 1.45	[6]
10097375	5612 ± 90	4.32 ± 0.17	0.10 ± 0.09			
10752443	6646 ± 165	4.06 ± 0.23	-0.29 ± 0.15			
10873176	6058 ± 99	4.05 ± 0.21	-0.68 ± 0.20	49.6 ± 0.9	821 ± 27	[1]
10919121	5577 ± 117	4.16 ± 0.21	0.22 ± 0.11			
11136690	6032 ± 136	4.16 ± 0.21	-0.81 ± 0.31			
11466403	5598 ± 90	4.16 ± 0.19	-0.22 ± 0.10	8.024 ± 0.80	84.626 ± 8.46	[5]

Reference: [1] Chaplin et al. (2014); [2] Huber et al. (2013); [3] Mosser et al. (2012); [4] Appourchaux et al. (2012); [5] Stello et al. (2013); [6] Hekker et al. (2011).

Table 2 Input Parameters for Grid Calculation

$[\mathrm{Fe/H}]_{\mathrm{ini}}$ (dex)	–0.3 ∼ +0.4	δ[Fe/H] (dex)	0.1
Z_{ini} (dex)	0.0085 ∼ 0.0400		
M ($M_\odot$)	0.8 ∼ 2.5	δM ($M_\odot$)	0.02
α	1.75, 1.842, 1.95	$\delta\alpha$	0.1

$1.1\,M_\odot$, using the formulation of Thoul et al. (1994). For grids with an initial mass between 1.1 and $1.2\,M_\odot$, both models with and without atomic diffusion are calculated. The outer convective zone is treated according to mixing-length theory (Böhm-Vitense 1958) and the influence of overshooting convection is ignored. To account for the uncertain mixing-length parameter, α_{MLT}, three sets of model grids are calculated, each with an α_{MLT} of 1.75, 1.84 and 1.95, respectively; the solar-calibrated value is $\alpha_{\mathrm{MLT}} = 1.84$.

We calculate stellar evolution models with [Fe/H] in the range -0.3 – $0.4\,\mathrm{dex}$ in steps of $0.1\,\mathrm{dex}$. We assume that $[\mathrm{Fe/H}] = 0$ corresponds to the solar abundance ($(Z/X)_\odot = 0.0231$) as determined by Grevesse & Sauval (1998) and that these models have a helium abundance of $Y = 0.248$. The helium abundance for models with other values of metallicity is determined assuming a chemical evolution model $Y_{\mathrm{ini}} = 0.248 + \Delta Y/\Delta Z \times Z$, where $\Delta Y/\Delta Z$=1.33. For each [Fe/H], the ratio of heavy-elements to hydrogen as a mass fraction is estimated through the formula

$$[\mathrm{Fe/H}] = \log\left(\frac{Z}{X}\right) - \log\left(\frac{Z}{X}\right)_\odot . \quad (1)$$

Our models have masses in the range 0.8–$2.5\,M_\odot$, in steps of $0.02\,M_\odot$. The evolution tracks are constructed from the pre-main sequence to the base of the red-giant branch (RGB). A summary of the adopted input parameters is given in Table 2.

Figure 1 shows the evolution tracks in the T_{eff}–$\log g$ plane and the position of the 179 MSTO star candidates, with parameters derived by the LSP3. The error bars represent the error of T_{eff} and $\log g$ derived from the LSP3 separately. The figure indicates that most of the MSTO star candidates are located around the MSTO stage.

3.2 Methodology

Usually, stellar parameters of field MSTO stars are determined by comparing theoretical models with atmospheric parameters such as T_{eff} and [Fe/H] derived from either photometry or spectroscopy. Low-mass main-sequence stars and some sub-giants show rich spectra of solar-like oscillations, small amplitude pulsations which are excited and damped intrinsically by convection in the outer envelope. The large frequency spacing, $\Delta\nu$, is formally related to the mean density of a star (Christensen-Dalsgaard 1993). The frequency of maximum power of the oscillation ν_{max} is related to the acoustic cutoff frequency of a star (e.g. Kjeldsen & Bedding 1995; Bedding & Kjeldsen 2003; Chaplin et al. 2008). Both $\Delta\nu$ and ν_{max} are sensitive to the structure of stars, and thus are indicators of the evolutionary stage.

Under the constraints of atmospheric parameters (T_{eff} and [Fe/H]) and seismic properties ($\Delta\nu$ and ν_{max}) listed in Table 1, we use the likelihood method of Basu et al. (2010) to find the best-fit models.

Given the observed and model parameters, the likelihood is:

$$L_{\mathrm{T_{eff}}} = \frac{1}{\sqrt{2\pi}\sigma_{\mathrm{T_{eff}}}} \exp\left(\frac{-(T_{\mathrm{eff_{obs}}} - T_{\mathrm{eff_{model}}})^2}{2\sigma^2_{\mathrm{T_{eff}}}}\right), \quad (2)$$

$$L_{[\mathrm{Fe/H}]} = \frac{1}{\sqrt{2\pi}\sigma_{[\mathrm{Fe/H}]}} \times \exp\left(\frac{-([\mathrm{Fe/H}]_{\mathrm{obs}} - [\mathrm{Fe/H}]_{\mathrm{model}})^2}{2\sigma^2_{[\mathrm{Fe/H}]}}\right), \quad (3)$$

$$L_{\Delta\nu} = \frac{1}{\sqrt{2}\pi\sigma_{\Delta\nu}} \exp\left(\frac{-(\Delta\nu_{\mathrm{obs}} - \Delta\nu_{\mathrm{model}})^2}{2\sigma^2_{\Delta\nu}}\right), \quad (4)$$

$$L_{\nu_{\mathrm{max}}} = \frac{1}{\sqrt{2}\pi\sigma_{\nu_{\mathrm{max}}}} \times \exp\left(\frac{-(\nu_{\mathrm{max,obs}} - \nu_{\mathrm{max,model}})^2}{2\sigma^2_{\nu_{\mathrm{max}}}}\right). \quad (5)$$

The combined likelihood is

$$L = L_{\Delta\nu}\, L_{\nu_{\mathrm{max}}}\, L_{\mathrm{T_{eff}}}\, L_{[\mathrm{Fe/H}]}. \quad (6)$$

Note that we do not consider the likelihood function for $\log g$ because the LSP3 estimates of this quantity may have large systematic errors. We assume that the normalized probability of each model p_i is

$$p_i = \frac{L_i}{\sum_{i=1}^{N_{\mathrm{m}}} L_i}, \quad (7)$$

where N_{m} is the total number of models. This normalized probability is a measurement of how well each

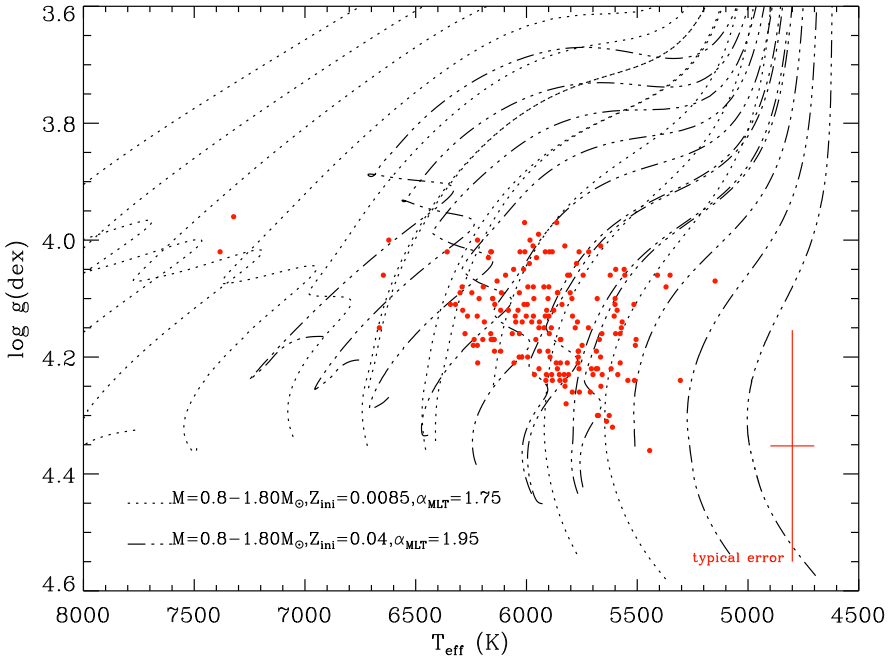

Fig. 1 MSTO stars and evolution tracks in the $T_{\rm eff}$–$\log g$ plane. The *black dotted lines* and *dash dotted lines* represent the stellar tracks with masses between 0.8 and 1.8 $M_{\odot}$, $Z_{\rm ini}$ between 0.0085 and 0.04 and $\alpha_{\rm MLT}$ between 1.75 and 1.95. The *red filled circles* represent the 179 MSTO stars with parameters derived by the LSP3, listed in Table 1. Typical error bars are presented in the *bottom-right corner* of the figure.

model in the set matches the parameters of an observed star. Similar to Kallinger et al. (2010), we use the integral probability to estimate the best-fitted parameter and its error. For each parameter, the best-fitted parameter respects the value that has an integral probability of 0.5, and the 1σ error is given.

4 RESULTS AND DISCUSSION

Among the 179 MSTO star candidates, stellar parameters for 150 of them are successfully derived, and are listed in Table 3, while the remaining 29 stars are falling outside of our model grids. For the 29 remaining stars, 25 stars are RGB stars according to their asteroseismic characteristics and the other four stars are metal-poor stars with $[{\rm Fe/H}] < -0.3\,{\rm dex}$.

Figure 2 illustrates distributions of the derived mass, age and metallicity for the 150 MSTO star candidates. Their masses are in the range of 0.8 – $1.5\,M_{\odot}$ and peak at about $1.1\,M_{\odot}$. The ages are widely distributed in the range of 0 – $13\,{\rm Gyr}$, mostly in 2 – $8\,{\rm Gyr}$. The metallicities are distributed in the range of -0.3 – $0.3\,{\rm dex}$, with a moderate peak near the solar value. Moreover, the typical uncertainties in $T_{\rm eff}$, $\log g$, [Fe/H], M and R are $60\,{\rm K}$, $0.009\,{\rm dex}$, $0.1\,{\rm dex}$, $0.04\,M_{\odot}$ and $0.03\,R_{\odot}$, respectively. The uncertainty in $\log g$ is much smaller than that yielded by the LSP3 from the LAMOST spectra. Uncertainties in the stellar age vary from $0.4\,{\rm Gyr}$ for young stars to $1.3\,{\rm Gyr}$ for old stars, corresponding to a relative error of about 9%–10%.

In fact, part of the stellar parameters for those 150 MSTO star candidates are also provided by Huber et al. (2014). Based on the Dartmouth Stellar Evolution Database (DSEP, Dotter et al. 2008), Huber et al. (2014) derived fundamental parameters using the asteroseismic quantities and atmospheric parameters in the *Kepler* input catalog (KIC), which are estimated from photometry for most stars, but they did not provide ages. By comparing the $\log g$, M and R derived by Huber et al. (2014) with those of our work in Figure 3, we find that our estimates of $\log g$ are very consistent with those of Huber et al., which yield a mean difference of only $0.0002\,{\rm dex}$ and a standard deviation of $0.013\,{\rm dex}$. However, there are systematic deviations of R and M between our estimates and those of Huber et al. Our values are systematically smaller than those of Huber et al., and the deviations increase with increasing R and M. A typical difference in R is 0.025 – $0.05\,R_{\odot}$ for stars with $R \sim 2.0$ $R_{\odot}$, and a typical difference of M is 0.1 – $0.2\,M_{\odot}$ for

Table 3 Fundamental Parameters of 150 Stars

Star KIC	$T_{\rm eff}$ (K)	$\log g$ (dex)	[Fe/H] (dex)	M ($M_\odot$)	R ($R_\odot$)	Age (Gyr)	L ($L_\odot$)
MSTO stars							
1725815	6225^{+77}_{-93}	$3.966^{+0.008}_{-0.011}$	$0.01^{+0.10}_{-0.10}$	$1.28^{+0.04}_{-0.04}$	$1.95^{+0.03}_{-0.03}$	$3.94^{+0.55}_{-0.34}$	$5.14^{+0.36}_{-0.38}$
2865774	5807^{+52}_{-60}	$4.022^{+0.017}_{-0.017}$	$0.10^{+0.03}_{-0.08}$	$1.12^{+0.04}_{-0.04}$	$1.71^{+0.04}_{-0.04}$	$7.03^{+0.69}_{-0.76}$	$2.99^{+0.19}_{-0.16}$
2998253	6107^{+62}_{-56}	$4.214^{+0.018}_{-0.016}$	$0.10^{+0.10}_{-0.11}$	$1.16^{+0.02}_{-0.04}$	$1.39^{+0.03}_{-0.04}$	$5.01^{+0.81}_{-0.61}$	$2.42^{+0.17}_{-0.15}$
3112152	5980^{+53}_{-62}	$4.029^{+0.013}_{-0.013}$	$-0.02^{+0.02}_{-0.07}$	$1.14^{+0.04}_{-0.04}$	$1.71^{+0.03}_{-0.03}$	$6.04^{+0.74}_{-0.66}$	$3.37^{+0.20}_{-0.20}$
3123191	6134^{+75}_{-54}	$4.217^{+0.012}_{-0.012}$	$-0.02^{+0.03}_{-0.10}$	$1.12^{+0.02}_{-0.04}$	$1.37^{+0.02}_{-0.02}$	$5.16^{+0.61}_{-0.66}$	$2.39^{+0.13}_{-0.11}$
3241581	5580^{+53}_{-54}	$4.386^{+0.007}_{-0.008}$	$0.34^{+0.11}_{-0.15}$	$1.02^{+0.04}_{-0.04}$	$1.08^{+0.02}_{-0.01}$	$6.39^{+1.93}_{-1.34}$	$1.02^{+0.05}_{-0.06}$
3656476	5543^{+75}_{-48}	$4.224^{+0.004}_{-0.006}$	$0.32^{+0.10}_{-0.10}$	$1.04^{+0.02}_{-0.04}$	$1.31^{+0.01}_{-0.01}$	$9.69^{+1.10}_{-1.59}$	$1.46^{+0.09}_{-0.08}$
3967859	5890^{+56}_{-57}	$4.218^{+0.015}_{-0.015}$	$-0.24^{+0.01}_{-0.10}$	$0.94^{+0.04}_{-0.04}$	$1.25^{+0.03}_{-0.03}$	$9.76^{+1.90}_{-1.10}$	$1.70^{+0.12}_{-0.11}$
4141376	5898^{+58}_{-53}	$4.404^{+0.006}_{-0.007}$	$-0.29^{+0.11}_{-0.010}$	$0.92^{+0.04}_{-0.02}$	$1.01^{+0.01}_{-0.01}$	$6.66^{+1.71}_{-1.37}$	$1.11^{+0.07}_{-0.06}$
4252818	5682^{+55}_{-57}	$4.065^{+0.019}_{-0.019}$	$0.11^{+0.10}_{-0.10}$	$1.06^{+0.02}_{-0.04}$	$1.58^{+0.05}_{-0.05}$	$8.75^{+1.23}_{-0.79}$	$2.35^{+0.19}_{-0.17}$
4465324	5776^{+70}_{-71}	$4.188^{+0.012}_{-0.013}$	$0.09^{+0.10}_{-0.10}$	$1.04^{+0.04}_{-0.04}$	$1.36^{+0.03}_{-0.03}$	$8.44^{+1.61}_{-1.19}$	$1.85^{+0.14}_{-0.13}$
4543171	5896^{+61}_{-68}	$4.101^{+0.008}_{-0.009}$	$0.20^{+0.10}_{-0.10}$	$1.16^{+0.02}_{-0.04}$	$1.59^{+0.02}_{-0.02}$	$6.05^{+0.91}_{-0.58}$	$2.74^{+0.15}_{-0.17}$
4554830	5510^{+49}_{-51}	$4.180^{+0.007}_{-0.007}$	$0.33^{+0.01}_{-0.01}$	$1.02^{+0.04}_{-0.02}$	$1.37^{+0.02}_{-0.02}$	$10.26^{+1.06}_{-1.01}$	$1.56^{+0.08}_{-0.08}$
4646780	6360^{+59}_{-73}	$3.994^{+0.014}_{-0.014}$	$-0.20^{+0.10}_{-0.10}$	$1.20^{+0.04}_{-0.04}$	$1.84^{+0.04}_{-0.04}$	$4.22^{+0.47}_{-0.47}$	$4.97^{+0.30}_{-0.35}$
4739932	5837^{+59}_{-55}	$4.003^{+0.011}_{-0.012}$	$0.13^{+0.07}_{-0.04}$	$1.16^{+0.04}_{-0.02}$	$1.79^{+0.03}_{-0.03}$	$6.25^{+0.60}_{-0.47}$	$3.34^{+0.17}_{-0.17}$
4755204	5925^{+54}_{-58}	$4.082^{+0.009}_{-0.008}$	$0.10^{+0.10}_{-0.10}$	$1.14^{+0.04}_{-0.04}$	$1.61^{+0.02}_{-0.02}$	$6.20^{+1.02}_{-0.63}$	$2.87^{+0.16}_{-0.15}$
4842436	5779^{+48}_{-59}	$4.091^{+0.018}_{-0.016}$	$0.20^{+0.10}_{-0.10}$	$1.12^{+0.02}_{-0.02}$	$1.58^{+0.03}_{-0.02}$	$7.45^{+0.73}_{-0.95}$	$2.50^{+0.15}_{-0.14}$
4914423	5860^{+55}_{-54}	$4.166^{+0.008}_{-0.010}$	$0.19^{+0.01}_{-0.10}$	$1.12^{+0.02}_{-0.04}$	$1.45^{+0.02}_{-0.02}$	$6.52^{+0.98}_{-0.63}$	$2.24^{+0.11}_{-0.11}$
4914923	5785^{+44}_{-50}	$4.208^{+0.004}_{-0.004}$	$0.20^{+0.01}_{-0.02}$	$1.10^{+0.02}_{-0.04}$	$1.37^{+0.01}_{-0.01}$	$7.11^{+0.90}_{-0.80}$	$1.89^{+0.07}_{-0.12}$
4947253	5903^{+57}_{-59}	$3.917^{+0.009}_{-0.010}$	$-0.06^{+0.06}_{-0.04}$	$1.18^{+0.02}_{-0.04}$	$1.97^{+0.03}_{-0.03}$	$5.58^{+0.45}_{-0.37}$	$4.25^{+0.24}_{-0.24}$
5094751	5833^{+58}_{-56}	$4.215^{+0.011}_{-0.010}$	$-0.02^{+0.10}_{-0.10}$	$1.04^{+0.04}_{-0.04}$	$1.33^{+0.02}_{-0.02}$	$7.77^{+1.16}_{-1.22}$	$1.83^{+0.11}_{-0.11}$
5095850	6647^{+66}_{-72}	$3.883^{+0.015}_{-0.016}$	$0.09^{+0.10}_{-0.10}$	$1.60^{+0.12}_{-0.04}$	$2.42^{+0.07}_{-0.06}$	$1.84^{+0.20}_{-0.42}$	$10.29^{+0.78}_{-0.73}$
5511081	5843^{+50}_{-61}	$4.013^{+0.024}_{-0.023}$	$0.02^{+0.07}_{-0.02}$	$1.10^{+0.06}_{-0.02}$	$1.73^{+0.05}_{-0.06}$	$7.04^{+0.62}_{-0.92}$	$3.13^{+0.21}_{-0.24}$
5512589	5733^{+51}_{-57}	$4.055^{+0.006}_{-0.006}$	$0.20^{+0.02}_{-0.07}$	$1.10^{+0.04}_{-0.02}$	$1.64^{+0.02}_{-0.01}$	$7.80^{+0.58}_{-0.72}$	$2.62^{+0.13}_{-0.13}$
5636956	6243^{+50}_{-72}	$3.969^{+0.008}_{-0.008}$	$0.20^{+0.08}_{-0.10}$	$1.36^{+0.04}_{-0.02}$	$2.01^{+0.03}_{-0.02}$	$3.25^{+0.45}_{-0.26}$	$5.65^{+0.31}_{-0.37}$
5686856	5882^{+63}_{-50}	$3.998^{+0.008}_{-0.007}$	$0.09^{+0.04}_{-0.06}$	$1.16^{+0.04}_{-0.04}$	$1.79^{+0.02}_{-0.03}$	$6.26^{+0.53}_{-0.53}$	$3.46^{+0.17}_{-0.15}$
5689219	6373^{+51}_{-60}	$4.039^{+0.009}_{-0.008}$	$-0.29^{+0.07}_{-0.04}$	$1.16^{+0.02}_{-0.06}$	$1.71^{+0.02}_{-0.03}$	$4.64^{+0.85}_{-0.41}$	$4.06^{+0.17}_{-0.20}$
5780885	5987^{+54}_{-69}	$3.966^{+0.015}_{-0.014}$	$0.20^{+0.10}_{-0.07}$	$1.26^{+0.02}_{-0.04}$	$1.93^{+0.04}_{-0.04}$	$4.84^{+0.40}_{-0.38}$	$4.31^{+0.25}_{-0.28}$
5961597	6338^{+38}_{-62}	$4.034^{+0.005}_{-0.006}$	$0.20^{+0.10}_{-0.10}$	$1.46^{+0.02}_{-0.04}$	$1.92^{+0.02}_{-0.02}$	$2.32^{+0.22}_{-0.18}$	$5.29^{+0.21}_{-0.16}$
6196457	5865^{+54}_{-51}	$4.055^{+0.009}_{-0.009}$	$0.20^{+0.10}_{-0.08}$	$1.16^{+0.02}_{-0.02}$	$1.69^{+0.02}_{-0.02}$	$6.08^{+0.81}_{-0.39}$	$3.03^{+0.22}_{-0.16}$
6268648	6033^{+67}_{-60}	$4.198^{+0.012}_{-0.012}$	$-0.25^{+0.10}_{-0.10}$	$1.00^{+0.04}_{-0.04}$	$1.33^{+0.02}_{-0.02}$	$7.46^{+0.97}_{-1.02}$	$2.10^{+0.13}_{-0.13}$
6521045	5816^{+50}_{-55}	$4.127^{+0.006}_{-0.007}$	$0.19^{+0.01}_{-0.09}$	$1.10^{+0.04}_{-0.02}$	$1.51^{+0.02}_{-0.02}$	$7.18^{+0.85}_{-0.90}$	$2.36^{+0.11}_{-0.13}$
6593461	5660^{+48}_{-53}	$4.216^{+0.011}_{-0.012}$	$0.18^{+0.01}_{-0.01}$	$1.04^{+0.02}_{-0.02}$	$1.32^{+0.02}_{-0.02}$	$8.86^{+1.38}_{-1.33}$	$1.64^{+0.10}_{-0.09}$
6605673	6010^{+58}_{-61}	$4.051^{+0.007}_{-0.007}$	$-0.24^{+0.03}_{-0.09}$	$1.04^{+0.04}_{-0.02}$	$1.61^{+0.02}_{-0.02}$	$7.20^{+0.70}_{-0.96}$	$3.03^{+0.17}_{-0.17}$
6689943	5947^{+51}_{-53}	$4.164^{+0.008}_{-0.010}$	$0.10^{+0.01}_{-0.01}$	$1.12^{+0.04}_{-0.02}$	$1.46^{+0.02}_{-0.02}$	$6.01^{+0.75}_{-0.79}$	$2.42^{+0.11}_{-0.11}$
6853020	6171^{+62}_{-64}	$3.956^{+0.012}_{-0.012}$	$0.10^{+0.10}_{-0.10}$	$1.30^{+0.04}_{-0.02}$	$2.00^{+0.04}_{-0.04}$	$3.90^{+0.31}_{-0.43}$	$5.20^{+0.29}_{-0.29}$
7133688	6314^{+54}_{-73}	$4.013^{+0.016}_{-0.015}$	$0.10^{+0.10}_{-0.10}$	$1.34^{+0.08}_{-0.04}$	$1.90^{+0.05}_{-0.05}$	$3.33^{+0.46}_{-0.83}$	$5.16^{+0.36}_{-0.42}$
7383120	6106^{+50}_{-76}	$4.196^{+0.011}_{-0.012}$	$-0.04^{+0.10}_{-0.10}$	$1.08^{+0.04}_{-0.02}$	$1.38^{+0.03}_{-0.02}$	$6.08^{+0.87}_{-0.87}$	$2.24^{+0.12}_{-0.13}$
7429287	5625^{+55}_{-79}	$4.059^{+0.008}_{-0.007}$	$-0.29^{+0.10}_{-0.09}$	$0.88^{+0.02}_{-0.04}$	$1.45^{+0.02}_{-0.02}$	$14.03^{+0.37}_{-1.18}$	$1.89^{+0.11}_{-0.10}$
7591963	5888^{+69}_{-53}	$3.987^{+0.008}_{-0.008}$	$0.12^{+0.08}_{-0.03}$	$1.18^{+0.02}_{-0.04}$	$1.83^{+0.03}_{-0.02}$	$5.85^{+0.53}_{-0.40}$	$3.62^{+0.22}_{-0.16}$
7680114	5815^{+61}_{-55}	$4.182^{+0.007}_{-0.007}$	$0.19^{+0.10}_{-0.10}$	$1.10^{+0.02}_{-0.04}$	$1.41^{+0.02}_{-0.02}$	$7.21^{+0.99}_{-1.10}$	$2.05^{+0.12}_{-0.12}$
7833440	6050^{+62}_{-61}	$4.034^{+0.009}_{-0.009}$	$-0.29^{+0.08}_{-0.04}$	$1.06^{+0.04}_{-0.02}$	$1.65^{+0.02}_{-0.02}$	$6.70^{+0.65}_{-0.85}$	$3.29^{+0.21}_{-0.19}$
7910848	5959^{+58}_{-56}	$4.106^{+0.010}_{-0.010}$	$0.12^{+0.08}_{-0.02}$	$1.16^{+0.02}_{-0.04}$	$1.58^{+0.02}_{-0.02}$	$5.84^{+0.89}_{-0.51}$	$2.84^{+0.14}_{-0.15}$
8012842	5713^{+80}_{-48}	$4.250^{+0.011}_{-0.011}$	$0.18^{+0.10}_{-0.10}$	$1.06^{+0.02}_{-0.02}$	$1.29^{+0.02}_{-0.02}$	$7.60^{+1.13}_{-1.08}$	$1.59^{+0.11}_{-0.09}$
8298626	5980^{+51}_{-78}	$4.224^{+0.009}_{-0.009}$	$-0.02^{+0.10}_{-0.10}$	$1.08^{+0.02}_{-0.04}$	$1.33^{+0.02}_{-0.02}$	$6.40^{+0.96}_{-1.06}$	$2.02^{+0.12}_{-0.11}$
8349582	5602^{+52}_{-52}	$4.168^{+0.009}_{-0.009}$	$0.19^{+0.14}_{-0.10}$	$1.04^{+0.04}_{-0.04}$	$1.40^{+0.02}_{-0.02}$	$9.70^{+1.10}_{-1.68}$	$1.73^{+0.09}_{-0.10}$
8367710	6151^{+70}_{-102}	$3.969^{+0.010}_{-0.009}$	$0.02^{+0.08}_{-0.10}$	$1.24^{+0.04}_{-0.04}$	$1.92^{+0.03}_{-0.03}$	$4.41^{+0.70}_{-0.46}$	$4.75^{+0.30}_{-0.40}$
8391021	6119^{+51}_{-69}	$4.150^{+0.008}_{-0.008}$	$-0.27^{+0.03}_{-0.09}$	$1.06^{+0.04}_{-0.04}$	$1.44^{+0.02}_{-0.02}$	$6.08^{+1.15}_{-0.62}$	$2.60^{+0.14}_{-0.16}$
8420801	6169^{+57}_{-67}	$4.069^{+0.013}_{-0.013}$	$0.10^{+0.10}_{-0.10}$	$1.24^{+0.02}_{-0.04}$	$1.71^{+0.03}_{-0.03}$	$4.47^{+0.57}_{-0.43}$	$3.78^{+0.23}_{-0.22}$
8491374	6212^{+56}_{-66}	$3.978^{+0.017}_{-0.017}$	$0.01^{+0.10}_{-0.10}$	$1.26^{+0.04}_{-0.02}$	$1.92^{+0.05}_{-0.05}$	$4.11^{+0.36}_{-0.32}$	$4.90^{+0.31}_{-0.34}$

Table 3 *Continued.*

Star KIC	$T_{\rm eff}$ (K)	$\log g$ (dex)	[Fe/H] (dex)	M ($M_\odot$)	R ($R_\odot$)	Age (Gyr)	L ($L_\odot$)
8493800	5917^{+59}_{-49}	$4.184^{+0.009}_{-0.008}$	$-0.02^{+0.10}_{-0.01}$	$1.10^{+0.02}_{-0.04}$	$1.40^{+0.02}_{-0.02}$	$6.32^{+1.17}_{-0.61}$	$2.19^{+0.10}_{-0.11}$
8494142	5968^{+49}_{-67}	$4.006^{+0.007}_{-0.007}$	$-0.01^{+0.02}_{-0.08}$	$1.14^{+0.04}_{-0.04}$	$1.76^{+0.02}_{-0.02}$	$6.07^{+0.63}_{-0.82}$	$3.55^{+0.18}_{-0.20}$
8554498	5849^{+62}_{-52}	$4.012^{+0.008}_{-0.008}$	$0.14^{+0.06}_{-0.02}$	$1.18^{+0.02}_{-0.02}$	$1.78^{+0.02}_{-0.02}$	$6.10^{+0.58}_{-0.57}$	$3.32^{+0.18}_{-0.15}$
8776961	5832^{+52}_{-61}	$4.030^{+0.008}_{-0.008}$	$0.09^{+0.03}_{-0.08}$	$1.14^{+0.03}_{-0.03}$	$1.70^{+0.03}_{-0.03}$	$6.96^{+0.70}_{-0.97}$	$3.00^{+0.16}_{-0.15}$
8915084	5828^{+49}_{-58}	$4.146^{+0.009}_{-0.009}$	$0.19^{+0.10}_{-0.10}$	$1.10^{+0.04}_{-0.02}$	$1.48^{+0.02}_{-0.02}$	$7.04^{+0.88}_{-0.78}$	$2.27^{+0.11}_{-0.14}$
8938364	5639^{+59}_{-57}	$4.165^{+0.006}_{-0.007}$	$-0.11^{+0.01}_{-0.11}$	$0.92^{+0.02}_{-0.04}$	$1.31^{+0.02}_{-0.02}$	$13.27^{+1.38}_{-1.20}$	$1.57^{+0.09}_{-0.09}$
8956017	6230^{+61}_{-65}	$4.041^{+0.012}_{-0.012}$	$0.10^{+0.10}_{-0.10}$	$1.28^{+0.04}_{-0.04}$	$1.79^{+0.04}_{-0.03}$	$3.93^{+0.50}_{-0.47}$	$4.36^{+0.31}_{-0.27}$
8981766	6206^{+57}_{-69}	$4.056^{+0.008}_{-0.009}$	$0.20^{+0.10}_{-0.10}$	$1.30^{+0.12}_{-0.04}$	$1.79^{+0.06}_{-0.04}$	$3.73^{+0.60}_{-1.20}$	$4.27^{+0.40}_{-0.30}$
9005973	5824^{+63}_{-56}	$4.160^{+0.013}_{-0.012}$	$-0.01^{+0.01}_{-0.01}$	$1.04^{+0.04}_{-0.02}$	$1.41^{+0.02}_{-0.03}$	$8.02^{+1.40}_{-1.04}$	$2.07^{+0.13}_{-0.13}$
9446628	6147^{+67}_{-67}	$3.964^{+0.018}_{-0.018}$	$-0.08^{+0.08}_{-0.05}$	$1.20^{+0.04}_{-0.04}$	$1.90^{+0.05}_{-0.05}$	$4.83^{+0.54}_{-0.52}$	$4.61^{+0.38}_{-0.34}$
9451706	5936^{+63}_{-46}	$4.252^{+0.008}_{-0.008}$	$0.20^{+0.10}_{-0.10}$	$1.12^{+0.02}_{-0.02}$	$1.32^{+0.02}_{-0.02}$	$5.90^{+0.67}_{-0.79}$	$1.95^{+0.10}_{-0.09}$
9451741	5667^{+83}_{-47}	$4.243^{+0.009}_{-0.010}$	$0.18^{+0.01}_{-0.01}$	$1.04^{+0.04}_{-0.02}$	$1.28^{+0.02}_{-0.02}$	$8.09^{+1.51}_{-0.92}$	$1.55^{+0.09}_{-0.09}$
9697131	6161^{+56}_{-70}	$4.005^{+0.010}_{-0.009}$	$0.0^{+0.10}_{-0.10}$	$1.22^{+0.04}_{-0.04}$	$1.83^{+0.03}_{-0.03}$	$4.61^{+0.48}_{-0.38}$	$4.32^{+0.23}_{-0.28}$
9700430	5888^{+59}_{-57}	$4.147^{+0.009}_{-0.010}$	$0.19^{+0.01}_{-0.10}$	$1.12^{+0.04}_{-0.02}$	$1.49^{+0.02}_{-0.02}$	$6.43^{+0.81}_{-0.59}$	$2.40^{+0.12}_{-0.12}$
9754284	5955^{+50}_{-56}	$4.111^{+0.01}_{-0.011}$	$0.10^{+0.01}_{-0.01}$	$1.14^{+0.02}_{-0.04}$	$1.56^{+0.02}_{-0.02}$	$5.99^{+1.04}_{-0.59}$	$2.75^{+0.14}_{-0.13}$
9872292	6124^{+84}_{-56}	$4.030^{+0.011}_{-0.010}$	$0.00^{+0.10}_{-0.10}$	$1.18^{+0.02}_{-0.02}$	$1.74^{+0.02}_{-0.02}$	$5.17^{+0.52}_{-0.37}$	$3.83^{+0.28}_{-0.17}$
9962623	5687^{+58}_{-59}	$4.148^{+0.016}_{-0.015}$	$-0.01^{+0.01}_{-0.01}$	$0.98^{+0.04}_{-0.02}$	$1.39^{+0.03}_{-0.02}$	$10.45^{+1.20}_{-1.08}$	$1.82^{+0.11}_{-0.11}$
10019747	5591^{+48}_{-63}	$4.042^{+0.009}_{-0.009}$	$0.23^{+0.12}_{-0.01}$	$1.10^{+0.04}_{-0.02}$	$1.67^{+0.03}_{-0.03}$	$8.43^{+0.72}_{-1.15}$	$2.44^{+0.12}_{-0.14}$
10322381	6063^{+57}_{-60}	$4.187^{+0.019}_{-0.019}$	$-0.25^{+0.01}_{-0.10}$	$1.02^{+0.04}_{-0.04}$	$1.35^{+0.04}_{-0.04}$	$7.00^{+1.18}_{-0.90}$	$2.22^{+0.17}_{-0.16}$
10351059	6249^{+65}_{-66}	$4.061^{+0.010}_{-0.009}$	$0.20^{+0.10}_{-0.10}$	$1.32^{+0.12}_{-0.04}$	$1.79^{+0.05}_{-0.03}$	$3.48^{+0.50}_{-1.07}$	$4.44^{+0.31}_{-0.30}$
10398597	6167^{+59}_{-69}	$3.981^{+0.013}_{-0.012}$	$0.20^{+0.10}_{-0.10}$	$1.32^{+0.04}_{-0.06}$	$1.94^{+0.04}_{-0.04}$	$3.90^{+0.37}_{-0.44}$	$4.90^{+0.32}_{-0.30}$
10586004	5782^{+52}_{-61}	$4.079^{+0.008}_{-0.008}$	$0.20^{+0.10}_{-0.01}$	$1.12^{+0.04}_{-0.02}$	$1.61^{+0.02}_{-0.02}$	$7.18^{+0.86}_{-0.83}$	$2.61^{+0.15}_{-0.14}$
10732098	5772^{+53}_{-53}	$4.000^{+0.008}_{-0.007}$	$0.13^{+0.07}_{-0.03}$	$1.14^{+0.02}_{-0.04}$	$1.77^{+0.02}_{-0.02}$	$7.10^{+0.75}_{-0.87}$	$3.13^{+0.15}_{-0.15}$
10875245	5701^{+66}_{-53}	$4.189^{+0.016}_{-0.015}$	$0.19^{+0.14}_{-0.01}$	$1.08^{+0.02}_{-0.04}$	$1.39^{+0.03}_{-0.03}$	$7.79^{+1.11}_{-0.65}$	$1.84^{+0.11}_{-0.12}$
11188219	5800^{+47}_{-50}	$4.239^{+0.011}_{-0.009}$	$0.18^{+0.02}_{-0.01}$	$1.10^{+0.02}_{-0.04}$	$1.32^{+0.02}_{-0.02}$	$6.81^{+0.68}_{-0.73}$	$1.78^{+0.08}_{-0.11}$
11244118	5618^{+50}_{-60}	$4.087^{+0.006}_{-0.006}$	$0.34^{+0.10}_{-0.13}$	$1.10^{+0.04}_{-0.04}$	$1.58^{+0.02}_{-0.02}$	$8.06^{+0.95}_{-1.17}$	$2.24^{+0.13}_{-0.14}$
11506988	6216^{+65}_{-64}	$3.979^{+0.009}_{-0.009}$	$-0.20^{+0.10}_{-0.1}$	$1.16^{+0.04}_{-0.04}$	$1.83^{+0.03}_{-0.03}$	$4.97^{+0.45}_{-0.38}$	$4.49^{+0.26}_{-0.25}$
11507653	5854^{+51}_{-59}	$4.081^{+0.015}_{-0.015}$	$0.20^{+0.02}_{-0.01}$	$1.16^{+0.02}_{-0.04}$	$1.62^{+0.04}_{-0.04}$	$6.41^{+1.03}_{-0.65}$	$2.79^{+0.16}_{-0.17}$
11611414	6039^{+55}_{-59}	$4.055^{+0.018}_{-0.017}$	$-0.02^{+0.02}_{-0.07}$	$1.14^{+0.04}_{-0.04}$	$1.67^{+0.04}_{-0.04}$	$5.84^{+0.72}_{-0.72}$	$3.33^{+0.19}_{-0.22}$
11971746	5879^{+45}_{-79}	$4.228^{+0.011}_{-0.011}$	$0.21^{+0.08}_{-0.02}$	$1.13^{+0.02}_{-0.05}$	$1.35^{+0.02}_{-0.02}$	$6.44^{+0.67}_{-0.67}$	$1.94^{+0.10}_{-0.10}$
12265063	5963^{+51}_{-66}	$4.058^{+0.012}_{-0.011}$	$-0.02^{+0.03}_{-0.07}$	$1.12^{+0.04}_{-0.04}$	$1.64^{+0.03}_{-0.03}$	$6.45^{+0.73}_{-0.76}$	$3.05^{+0.18}_{-0.18}$
Main sequence stars							
3241581	5580^{+53}_{-54}	$4.386^{+0.007}_{-0.008}$	$0.34^{+0.02}_{-0.15}$	$1.02^{+0.04}_{-0.04}$	$1.08^{+0.02}_{-0.01}$	$6.39^{+1.93}_{-1.34}$	$1.02^{+0.05}_{-0.06}$
4349452	6159^{+67}_{-58}	$4.274^{+0.005}_{-0.005}$	$-0.01^{+0.01}_{-0.010}$	$1.14^{+0.02}_{-0.04}$	$1.29^{+0.01}_{-0.01}$	$4.10^{+0.85}_{-0.85}$	$2.15^{+0.13}_{-0.09}$
5088536	5818^{+50}_{-49}	$4.302^{+0.011}_{-0.008}$	$-0.11^{+0.05}_{-0.04}$	$0.94^{+0.04}_{-0.02}$	$1.15^{+0.01}_{-0.02}$	$9.68^{+0.97}_{-1.17}$	$1.34^{+0.08}_{-0.06}$
5253542	5649^{+73}_{-64}	$4.313^{+0.010}_{-0.009}$	$0.19^{+0.15}_{-0.10}$	$1.02^{+0.04}_{-0.04}$	$1.18^{+0.02}_{-0.02}$	$8.26^{+1.48}_{-1.70}$	$1.27^{+0.09}_{-0.08}$
6603624	5512^{+47}_{-46}	$4.319^{+0.006}_{-0.006}$	$0.32^{+0.10}_{-0.10}$	$1.00^{+0.02}_{-0.02}$	$1.15^{+0.01}_{-0.01}$	$9.93^{+1.16}_{-1.16}$	$1.09^{+0.05}_{-0.04}$
8394589	5976^{+74}_{-33}	$4.306^{+0.010}_{-0.009}$	$-0.32^{+0.11}_{-0.10}$	$0.94^{+0.04}_{-0.02}$	$1.14^{+0.01}_{-0.01}$	$8.53^{+1.13}_{-1.89}$	$1.48^{+0.10}_{-0.06}$
9116461	6217^{+56}_{-58}	$4.314^{+0.011}_{-0.011}$	$0.01^{+0.10}_{-0.1}$	$1.16^{+0.02}_{-0.04}$	$1.24^{+0.02}_{-0.02}$	$3.13^{+0.87}_{-0.73}$	$2.07^{+0.12}_{-0.10}$
10079226	5869^{+50}_{-80}	$4.369^{+0.008}_{-0.008}$	$0.21^{+0.01}_{-0.090}$	$1.08^{+0.04}_{-0.02}$	$1.13^{+0.01}_{-0.01}$	$3.99^{+1.17}_{-0.99}$	$1.37^{+0.07}_{-0.08}$
11133306	5894^{+80}_{-70}	$4.315^{+0.010}_{-0.009}$	$-0.01^{+0.01}_{-0.01}$	$1.04^{+0.02}_{-0.04}$	$1.18^{+0.02}_{-0.02}$	$6.20^{+2.02}_{-1.33}$	$1.52^{+0.09}_{-0.10}$
12068975	5929^{+69}_{-33}	$4.298^{+0.014}_{-0.010}$	$-0.32^{+0.10}_{-0.01}$	$0.92^{+0.04}_{-0.02}$	$1.14^{+0.02}_{-0.02}$	$9.45^{+1.22}_{-1.51}$	$1.43^{+0.09}_{-0.07}$
Giant stars							
2010607	6117^{+64}_{-64}	$3.819^{+0.018}_{-0.017}$	$0.10^{+0.10}_{-0.10}$	$1.42^{+0.04}_{-0.04}$	$2.44^{+0.08}_{-0.07}$	$2.99^{+0.21}_{-0.26}$	$7.58^{+0.49}_{-0.66}$
3344897	6234^{+69}_{-63}	$3.870^{+0.009}_{-0.008}$	$0.010^{+0.10}_{-0.010}$	$1.36^{+0.04}_{-0.04}$	$2.25^{+0.03}_{-0.03}$	$3.26^{+0.23}_{-0.23}$	$6.80^{+0.45}_{-0.37}$
3438633	6076^{+62}_{-57}	$3.950^{+0.013}_{-0.013}$	$-0.20^{+0.10}_{-0.01}$	$1.14^{+0.04}_{-0.02}$	$1.88^{+0.04}_{-0.04}$	$5.41^{+0.47}_{-0.43}$	$4.35^{+0.26}_{-0.23}$
3456181	6234^{+61}_{-59}	$3.926^{+0.008}_{-0.007}$	$0.01^{+0.10}_{-0.01}$	$1.30^{+0.04}_{-0.02}$	$2.07^{+0.02}_{-0.02}$	$3.72^{+0.29}_{-0.25}$	$5.82^{+0.28}_{-0.3}$
3942719	5665^{+53}_{-61}	$3.833^{+0.017}_{-0.019}$	$-0.25^{+0.02}_{-0.09}$	$1.08^{+0.04}_{-0.04}$	$2.09^{+0.07}_{-0.07}$	$6.38^{+0.86}_{-0.43}$	$4.04^{+0.34}_{-0.32}$
4049576	5810^{+55}_{-60}	$3.903^{+0.015}_{-0.015}$	$-0.17^{+0.03}_{-0.09}$	$1.10^{+0.02}_{-0.04}$	$1.94^{+0.05}_{-0.04}$	$6.65^{+0.51}_{-0.42}$	$3.89^{+0.29}_{-0.24}$
4143755	5683^{+56}_{-58}	$4.095^{+0.008}_{-0.008}$	$-0.40^{+0.10}_{-0.10}$	$0.84^{+0.02}_{-0.02}$	$1.37^{+0.02}_{-0.02}$	$14.11^{+1.30}_{-1.18}$	$1.77^{+0.09}_{-0.10}$
4165030	5678^{+56}_{-57}	$3.980^{+0.011}_{-0.010}$	$-0.27^{+0.09}_{-0.09}$	$0.94^{+0.02}_{-0.02}$	$1.65^{+0.03}_{-0.03}$	$10.40^{+0.90}_{-0.81}$	$2.54^{+0.16}_{-0.14}$

Table 3 *Continued.*

Star KIC	$T_{\rm eff}$ (K)	$\log g$ (dex)	[Fe/H] (dex)	M ($M_\odot$)	R ($R_\odot$)	Age (Gyr)	L ($L_\odot$)
4577484	5588^{+54}_{-57}	$3.861^{+0.013}_{-0.013}$	$0.24^{+0.05}_{-0.1}$	$1.26^{+0.02}_{-0.02}$	$2.19^{+0.05}_{-0.05}$	$5.10^{+0.38}_{-0.32}$	$4.21^{+0.25}_{-0.25}$
4672403	5764^{+59}_{-52}	$3.994^{+0.009}_{-0.009}$	$0.20^{+0.09}_{-0.06}$	$1.18^{+0.02}_{-0.04}$	$1.81^{+0.02}_{-0.03}$	$6.44^{+0.51}_{-0.40}$	$3.24^{+0.18}_{-0.16}$
4841753	5993^{+49}_{-61}	$3.906^{+0.016}_{-0.017}$	$0.20^{+0.10}_{-0.10}$	$1.30^{+0.04}_{-0.02}$	$2.12^{+0.05}_{-0.05}$	$4.14^{+0.29}_{-0.24}$	$5.23^{+0.30}_{-0.33}$
5095159	5298^{+71}_{-33}	$3.711^{+0.007}_{-0.008}$	$0.100^{+0.10}_{-0.10}$	$1.48^{+0.04}_{-0.06}$	$2.82^{+0.05}_{-0.04}$	$2.71^{+0.27}_{-0.25}$	$5.65^{+0.33}_{-0.31}$
5353186	6038^{+62}_{-62}	$3.885^{+0.010}_{-0.010}$	$0.10^{+0.10}_{-0.10}$	$1.32^{+0.04}_{-0.02}$	$2.19^{+0.03}_{-0.04}$	$3.89^{+0.23}_{-0.26}$	$5.73^{+0.35}_{-0.23}$
5523099	5507^{+57}_{-51}	$3.794^{+0.010}_{-0.010}$	$0.050^{+0.04}_{-0.08}$	$1.26^{+0.04}_{-0.04}$	$2.37^{+0.04}_{-0.05}$	$4.57^{+0.29}_{-0.27}$	$4.63^{+0.26}_{-0.26}$
5561278	5973^{+63}_{-55}	$3.960^{+0.011}_{-0.012}$	$-0.06^{+0.07}_{-0.04}$	$1.16^{+0.02}_{-0.04}$	$1.87^{+0.03}_{-0.03}$	$5.59^{+0.68}_{-0.34}$	$4.01^{+0.22}_{-0.18}$
6064910	6173^{+66}_{-60}	$3.818^{+0.009}_{-0.009}$	$-0.24^{+0.04}_{-0.07}$	$1.24^{+0.02}_{-0.04}$	$2.27^{+0.03}_{-0.04}$	$4.03^{+0.26}_{-0.42}$	$6.78^{+0.41}_{-0.39}$
6308642	5653^{+61}_{-47}	$3.797^{+0.010}_{-0.007}$	$-0.13^{+0.03}_{-0.07}$	$1.18^{+0.02}_{-0.02}$	$2.28^{+0.03}_{-0.03}$	$5.03^{+0.31}_{-0.27}$	$4.79^{+0.21}_{-0.20}$
6520835	6030^{+61}_{-59}	$3.895^{+0.007}_{-0.008}$	$0.00^{+0.10}_{-0.1}$	$1.24^{+0.02}_{-0.02}$	$2.09^{+0.02}_{-0.03}$	$4.63^{+0.32}_{-0.30}$	$5.11^{+0.29}_{-0.28}$
6587236	5916^{+58}_{-60}	$3.641^{+0.018}_{-0.017}$	$-0.29^{+0.09}_{-0.1}$	$1.42^{+0.04}_{-0.06}$	$2.98^{+0.08}_{-0.10}$	$2.43^{+0.36}_{-0.21}$	$9.83^{+0.71}_{-0.78}$
6592305	6005^{+59}_{-65}	$3.870^{+0.006}_{-0.006}$	$0.10^{+0.1}_{-0.1}$	$1.32^{+0.04}_{-0.04}$	$2.22^{+0.02}_{-0.03}$	$3.92^{+0.32}_{-0.25}$	$5.83^{+0.31}_{-0.30}$
6688822	5559^{+56}_{-53}	$3.860^{+0.009}_{-0.009}$	$0.28^{+0.10}_{-0.1}$	$1.28^{+0.02}_{-0.02}$	$2.21^{+0.03}_{-0.04}$	$5.06^{+0.30}_{-0.29}$	$4.18^{+0.22}_{-0.21}$
6693861	5756^{+52}_{-61}	$3.835^{+0.010}_{-0.010}$	$-0.25^{+0.02}_{-0.09}$	$1.10^{+0.02}_{-0.02}$	$2.10^{+0.03}_{-0.04}$	$6.06^{+0.32}_{-0.36}$	$4.37^{+0.23}_{-0.26}$
6766513	6169^{+56}_{-69}	$3.910^{+0.011}_{-0.011}$	$-0.10^{+0.10}_{-0.10}$	$1.24^{+0.04}_{-0.04}$	$2.06^{+0.04}_{-0.04}$	$4.24^{+0.36}_{-0.42}$	$5.51^{+0.35}_{-0.40}$
6863041	5623^{+53}_{-56}	$3.814^{+0.011}_{-0.010}$	$0.2^{+0.08}_{-0.1}$	$1.34^{+0.04}_{-0.02}$	$2.38^{+0.05}_{-0.04}$	$4.04^{+0.26}_{-0.24}$	$5.11^{+0.25}_{-0.27}$
7038145	5907^{+60}_{-73}	$3.820^{+0.006}_{-0.008}$	$0.01^{+0.10}_{-0.11}$	$1.32^{+0.02}_{-0.04}$	$2.34^{+0.03}_{-0.03}$	$3.79^{+0.42}_{-0.06}$	$6.03^{+0.29}_{-0.38}$
7107778	5136^{+61}_{-48}	$3.649^{+0.009}_{-0.009}$	$0.1^{+0.10}_{-0.100}$	$1.50^{+0.08}_{-0.10}$	$3.04^{+0.08}_{-0.09}$	$2.62^{+0.73}_{-0.42}$	$5.79^{+0.48}_{-0.50}$
7199397	5922^{+56}_{-61}	$3.757^{+0.008}_{-0.007}$	$-0.1^{+0.10}_{-0.10}$	$1.32^{+0.06}_{-0.02}$	$2.54^{+0.03}_{-0.04}$	$3.34^{+0.17}_{-0.14}$	$7.08^{+0.36}_{-0.29}$
7264595	5671^{+53}_{-47}	$3.698^{+0.011}_{-0.012}$	$-0.200^{+0.09}_{-0.100}$	$1.34^{+0.04}_{-0.04}$	$2.73^{+0.06}_{-0.06}$	$3.15^{+0.20}_{-0.27}$	$6.83^{+0.42}_{-0.31}$
7282890	6283^{+68}_{-73}	$3.874^{+0.008}_{-0.008}$	$0.2^{+0.10}_{-0.1}$	$1.48^{+0.03}_{-0.03}$	$2.33^{+0.03}_{-0.03}$	$2.69^{+0.22}_{-0.25}$	$7.57^{+0.51}_{-0.44}$
7386523	5845^{+56}_{-61}	$3.883^{+0.018}_{-0.018}$	$0.1^{+0.1}_{-0.1}$	$1.26^{+0.04}_{-0.04}$	$2.13^{+0.07}_{-0.06}$	$4.74^{+0.35}_{-0.43}$	$4.69^{+0.52}_{-0.29}$
7880676	6035^{+55}_{-64}	$3.944^{+0.009}_{-0.009}$	$0.14^{+0.06}_{-0.12}$	$1.26^{+0.04}_{-0.04}$	$1.99^{+0.03}_{-0.03}$	$4.50^{+0.42}_{-0.40}$	$4.76^{+0.25}_{-0.32}$
8016496	5996^{+60}_{-57}	$3.952^{+0.010}_{-0.009}$	$-0.06^{+0.07}_{-0.04}$	$1.18^{+0.02}_{-0.04}$	$1.90^{+0.03}_{-0.03}$	$5.46^{+0.47}_{-0.38}$	$4.18^{+0.22}_{-0.21}$
8019508	5995^{+63}_{-57}	$3.767^{+0.017}_{-0.018}$	$0.09^{+0.10}_{-0.10}$	$1.46^{+0.04}_{-0.04}$	$2.61^{+0.09}_{-0.07}$	$2.78^{+0.26}_{-0.18}$	$7.99^{+0.55}_{-0.55}$
8045442	5902^{+62}_{-58}	$3.669^{+0.010}_{-0.008}$	$0.09^{+0.1}_{-0.1}$	$1.62^{+0.02}_{-0.04}$	$3.08^{+0.05}_{-0.04}$	$1.99^{+0.10}_{-0.12}$	$10.32^{+0.57}_{-0.51}$
8493735	5887^{+58}_{-60}	$3.737^{+0.014}_{-0.01}$	$-0.1^{+0.1}_{-0.1}$	$1.36^{+0.04}_{-0.04}$	$2.61^{+0.06}_{-0.05}$	$3.18^{+0.17}_{-0.26}$	$7.37^{+0.42}_{-0.37}$
8621637	5676^{+55}_{-54}	$3.961^{+0.011}_{-0.010}$	$0.16^{+0.06}_{-0.06}$	$1.16^{+0.02}_{-0.04}$	$1.87^{+0.03}_{-0.03}$	$6.80^{+0.67}_{-0.55}$	$3.24^{+0.18}_{-0.18}$
8684730	5923^{+59}_{-64}	$3.927^{+0.012}_{-0.013}$	$0.10^{+0.10}_{-0.10}$	$1.24^{+0.04}_{-0.04}$	$2.02^{+0.04}_{-0.04}$	$4.94^{+0.38}_{-0.48}$	$4.44^{+0.40}_{-0.27}$
8802782	5868^{+53}_{-60}	$3.848^{+0.015}_{-0.015}$	$0.2^{+0.08}_{-0.1}$	$1.34^{+0.04}_{-0.02}$	$2.30^{+0.06}_{-0.05}$	$3.93^{+0.13}_{-0.35}$	$5.58^{+0.47}_{-0.26}$
8817551	5762^{+57}_{-54}	$3.818^{+0.008}_{-0.009}$	$0.2^{+0.08}_{-0.1}$	$1.36^{+0.04}_{-0.02}$	$2.39^{+0.04}_{-0.04}$	$3.79^{+0.23}_{-0.21}$	$5.70^{+0.29}_{-0.32}$
8868481	5589^{+56}_{-56}	$3.777^{+0.013}_{-0.013}$	$0.01^{+0.09}_{-0.01}$	$1.30^{+0.04}_{-0.02}$	$2.45^{+0.06}_{-0.06}$	$4.04^{+0.27}_{-0.40}$	$5.31^{+0.32}_{-0.30}$
9335972	5715^{+63}_{-53}	$3.851^{+0.009}_{-0.010}$	$0.15^{+0.05}_{-0.10}$	$1.26^{+0.04}_{-0.04}$	$2.22^{+0.04}_{-0.04}$	$4.78^{+0.30}_{-0.29}$	$4.74^{+0.24}_{-0.24}$
9592705	6068^{+52}_{-58}	$3.943^{+0.003}_{-0.004}$	$0.20^{+0.10}_{-0.10}$	$1.30^{+0.02}_{-0.02}$	$2.02^{+0.01}_{-0.02}$	$4.22^{+0.32}_{-0.43}$	$5.00^{+0.23}_{-0.24}$
9664694	6158^{+57}_{-63}	$3.808^{+0.011}_{-0.011}$	$0.00^{+0.10}_{-0.10}$	$1.38^{+0.02}_{-0.04}$	$2.43^{+0.04}_{-0.04}$	$3.14^{+0.20}_{-0.18}$	$7.57^{+0.42}_{-0.40}$
9696358	6000^{+55}_{-64}	$3.915^{+0.030}_{-0.030}$	$0.14^{+0.06}_{-0.11}$	$1.28^{+0.04}_{-0.04}$	$2.07^{+0.09}_{-0.09}$	$4.36^{+0.57}_{-0.39}$	$4.96^{+0.55}_{-0.43}$
9715099	6139^{+54}_{-67}	$3.799^{+0.009}_{-0.009}$	$0.10^{+0.1}_{-0.1}$	$1.46^{+0.04}_{-0.04}$	$2.53^{+0.04}_{-0.04}$	$2.74^{+0.24}_{-0.15}$	$8.08^{+0.43}_{-0.40}$
9757640	5516^{+50}_{-54}	$4.000^{+0.009}_{-0.008}$	$0.29^{+0.08}_{-0.06}$	$1.12^{+0.02}_{-0.04}$	$1.75^{+0.02}_{-0.02}$	$8.37^{+0.71}_{-0.95}$	$2.53^{+0.14}_{-0.08}$
9778067	5906^{+58}_{-60}	$3.884^{+0.014}_{-0.012}$	$-0.36^{+0.01}_{-0.02}$	$1.06^{+0.02}_{-0.02}$	$1.96^{+0.04}_{-0.04}$	$6.30^{+0.44}_{-0.13}$	$4.27^{+0.05}_{-0.26}$
9787965	6079^{+56}_{-69}	$3.929^{+0.016}_{-0.016}$	$0.01^{+0.10}_{-0.01}$	$1.26^{+0.02}_{-0.04}$	$2.02^{+0.05}_{-0.05}$	$4.50^{+0.41}_{-0.46}$	$4.99^{+0.37}_{-0.37}$
9791157	5841^{+58}_{-59}	$3.940^{+0.009}_{-0.009}$	$0.10^{+0.10}_{-0.05}$	$1.20^{+0.02}_{-0.04}$	$1.95^{+0.03}_{-0.03}$	$5.68^{+0.40}_{-0.40}$	$3.93^{+0.22}_{-0.22}$
10417911	5552^{+56}_{-53}	$3.955^{+0.017}_{-0.017}$	$0.25^{+0.04}_{-0.02}$	$1.16^{+0.02}_{-0.02}$	$1.89^{+0.05}_{-0.05}$	$7.02^{+0.66}_{-0.47}$	$3.02^{+0.19}_{-0.18}$
10727922	5999^{+58}_{-59}	$3.946^{+0.018}_{-0.019}$	$-0.11^{+0.02}_{-0.10}$	$1.14^{+0.04}_{-0.04}$	$1.89^{+0.05}_{-0.05}$	$5.76^{+0.54}_{-0.57}$	$4.14^{+0.26}_{-0.24}$
10731424	6162^{+62}_{-65}	$3.773^{+0.017}_{-0.019}$	$0.01^{+0.09}_{-0.01}$	$1.44^{+0.04}_{-0.04}$	$2.59^{+0.08}_{-0.08}$	$2.70^{+0.17}_{-0.24}$	$8.74^{+0.58}_{-0.71}$
10923629	6017^{+62}_{-60}	$3.819^{+0.010}_{-0.008}$	$0.2^{+0.08}_{-0.1}$	$1.42^{+0.04}_{-0.02}$	$2.45^{+0.03}_{-0.04}$	$3.05^{+0.19}_{-0.18}$	$7.07^{+0.38}_{-0.38}$
11083308	6032^{+59}_{-68}	$3.911^{+0.011}_{-0.011}$	$0.01^{+0.09}_{-0.01}$	$1.24^{+0.04}_{-0.02}$	$2.06^{+0.04}_{-0.04}$	$4.60^{+0.34}_{-0.49}$	$5.04^{+0.35}_{-0.30}$
11138101	6148^{+62}_{-62}	$3.835^{+0.014}_{-0.016}$	$0.01^{+0.09}_{-0.01}$	$1.36^{+0.04}_{-0.04}$	$2.34^{+0.06}_{-0.06}$	$3.31^{+0.21}_{-0.23}$	$7.08^{+0.49}_{-0.52}$
11193681	5594^{+66}_{-58}	$3.809^{+0.008}_{-0.007}$	$0.20^{+0.08}_{-0.01}$	$1.36^{+0.02}_{-0.04}$	$2.40^{+0.04}_{-0.03}$	$4.01^{+0.24}_{-0.33}$	$5.10^{+0.24}_{-0.26}$
11771760	5862^{+69}_{-62}	$3.674^{+0.010}_{-0.005}$	$0.01^{+0.09}_{-0.01}$	$1.54^{+0.04}_{-0.04}$	$2.99^{+0.05}_{-0.06}$	$2.17^{+0.20}_{-0.11}$	$9.53^{+0.47}_{-0.50}$
11817562	5974^{+60}_{-59}	$3.803^{+0.009}_{-0.009}$	$0.2^{+0.08}_{-0.01}$	$1.44^{+0.02}_{-0.02}$	$2.50^{+0.03}_{-0.04}$	$3.04^{+0.18}_{-0.16}$	$7.11^{+0.38}_{-0.35}$
11919192	6368^{+61}_{-69}	$3.890^{+0.009}_{-0.009}$	$-0.2^{+0.09}_{-0.1}$	$1.28^{+0.04}_{-0.02}$	$2.14^{+0.03}_{-0.03}$	$3.48^{+0.25}_{-0.32}$	$6.78^{+0.36}_{-0.43}$
12069127	6247^{+46}_{-75}	$3.891^{+0.009}_{-0.010}$	$0.1^{+0.1}_{-0.1}$	$1.42^{+0.02}_{-0.06}$	$2.23^{+0.03}_{-0.04}$	$3.02^{+0.39}_{-0.16}$	$6.83^{+0.28}_{-0.44}$

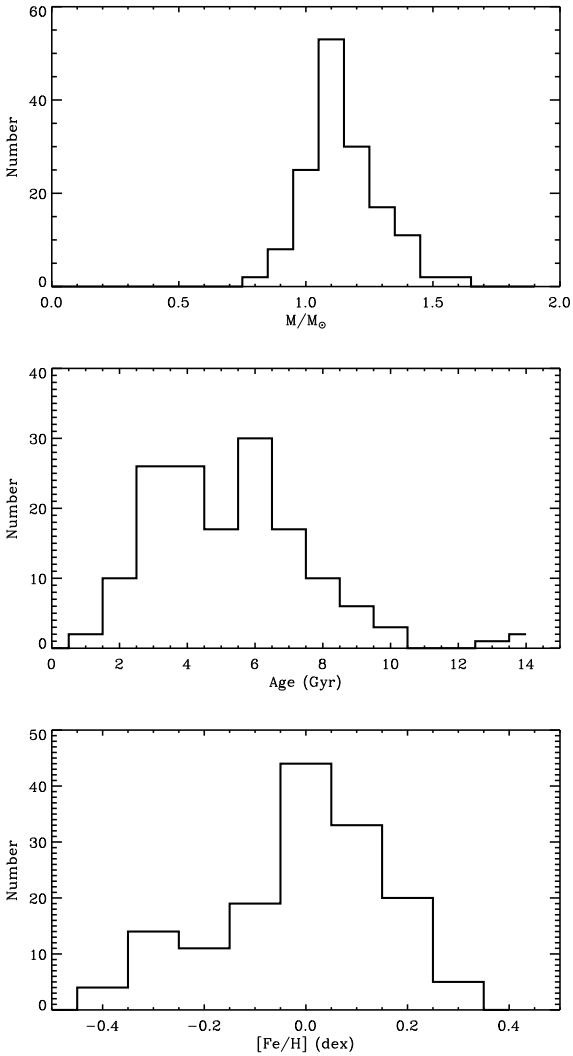

Fig. 2 Distribution of 150 MSTO stars with revised parameters. Different parameters lie in different panels, i.e., *top*: the distribution of masses, *middle*: the distribution of ages, *bottom*: the distribution of metallicities.

stars with $M \sim 1.5\ M_{\odot}$. Nevertheless, the dispersions of differences in R and M are small (after excluding systematic trends), with only $0.056\,R_{\odot}$ in R and $0.1\ M_{\odot}$ in M. The systematic trends of differences in R and M are mainly caused by systematic differences in the effective temperatures adopted.

In Figure 4, we compare $T_{\rm eff}$ derived by the LSP3 and those of Huber et al. The figure exhibits similar trends to those for mass in Figure 3. As expected, there is strong correlation between the differences in mass and the differences in effective temperatures. Because values of $T_{\rm eff}$ derived by the LSP3 are calibrated to the recently deduced metallicity-dependent color–temperature relation of Huang et al. (Huang et al. 2015), which is deduced based on stellar interferometry data sets, we believe our results on stellar mass are more reliable than those of Huber et al. In addition, the stellar metallicity could also affect the determination of stellar mass, but it has only a minor contribution compared to that from the effective temperature.

After that, in Figure 5, we compare age estimates of this work with those of Xiang et al. (2015b). The left panel shows that though ages for the majority of stars agree well with each other, there are a considerable fraction of stars for which our values are systematically much lower than those of Xiang et al. For stars older than 10 Gyr based on Xiang et al.'s age estimates, about half of them are actually younger than 7 Gyr according to our results. The right panel plots the distribution of the differences in age estimates. The distribution

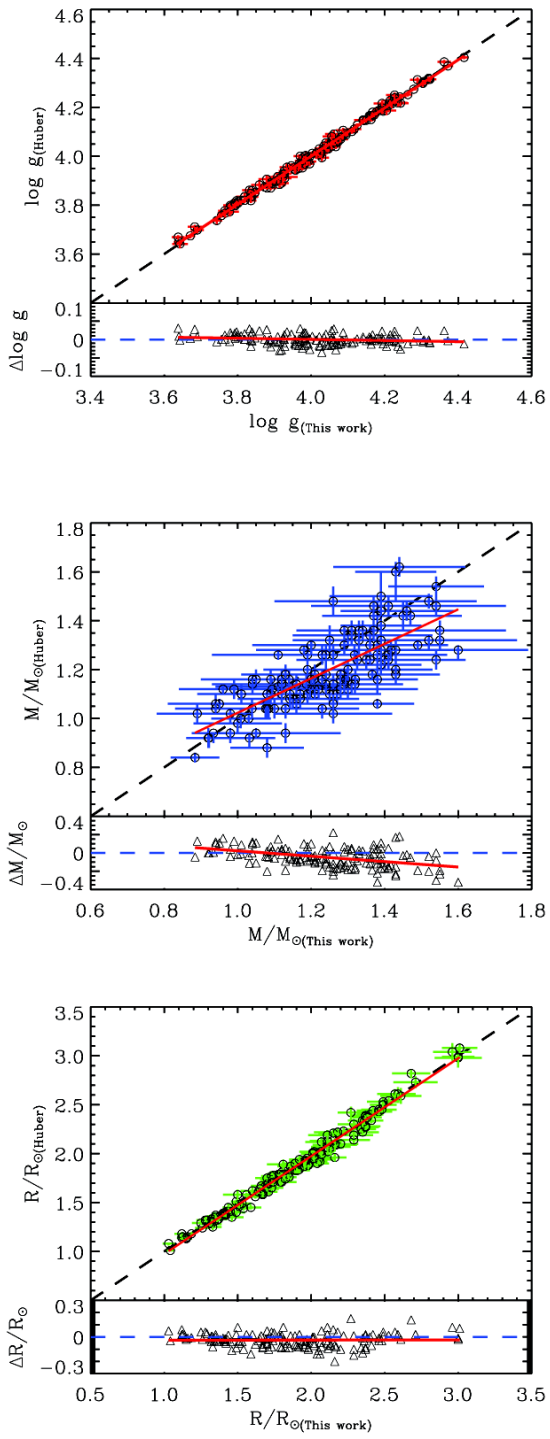

Fig. 3 Comparison of the results of Huber et al. (2014) and our work. Different parameters lie in different panels, i.e., *top*: gravity $\log g$, *middle*: mass M, and *bottom*: radius R. The *dashed line* shows the line of equality, and the *solid line* shows a least squares fitting of both results.

yields a mean difference of $0.53\,\mathrm{Gyr}$ (7%), and a dispersion of $2.71\,\mathrm{Gyr}$ (28%). It is found that the age discrepancies are mostly caused by systematic bias in the LSP3 $\log g$. For instance, for KIC 5523099, the LSP3 atmospheric parameters ($5513\,\mathrm{K}, 4.24\,\mathrm{dex}, 0.03\,\mathrm{dex}$) yield an age of $12.5\,\mathrm{Gyr}$, while our atmospheric parameters ($5507\,\mathrm{K}$, $3.79\,\mathrm{dex}$, $0.05\,\mathrm{dex}$) yield $4.6\,\mathrm{Gyr}$, which is $6.9\,\mathrm{Gyr}$ younger due to a $0.45\,\mathrm{dex}$ overestimate of the

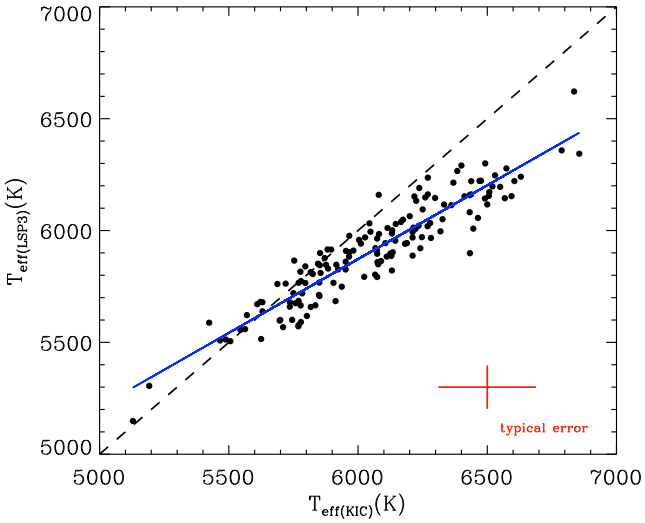

Fig. 4 Comparison of $T_{\rm eff}$ from LAMOST and *Kepler*. The *dashed line* shows the line of equality. The *blue solid line* shows least squares fitting of temperature. Typical error bars are presented in the *bottom-right corner* of the figure.

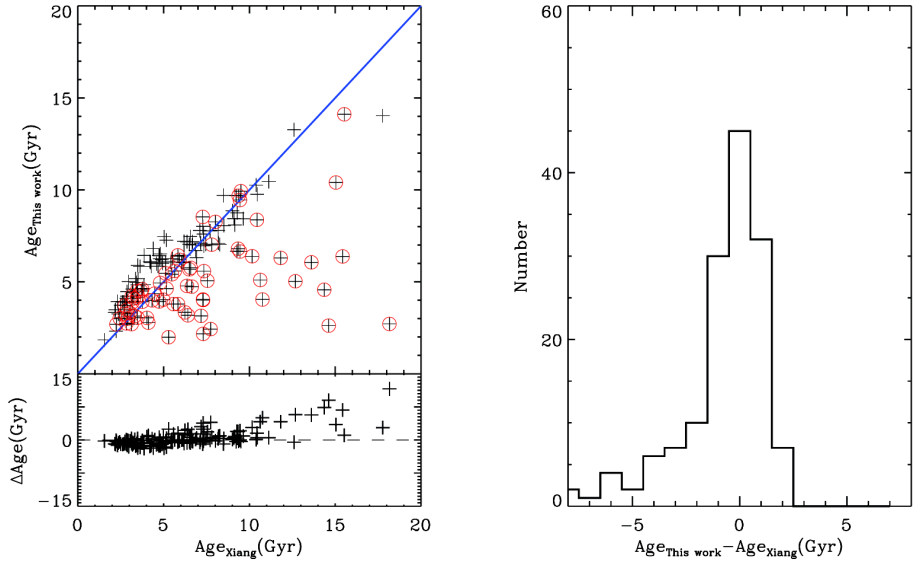

Fig. 5 Comparison of the ages from Xiang et al. (2015b) with our work. *Left panel*: comparison of age calculated by isochrone fitting (Xiang) with asteroseismology (our work). The *blue solid line* shows the line of equality. The *crosses* show the sample of 150 stars and red circles indicate the non-MSTO stars in our work. *Right panel*: histogram of differences in ages.

LSP3 $\log g$. As the uncertainty of the LSP3 $\log g$ is the main cause of the differences in stellar ages, in the left panel of Figure 6, we compare $\log g$ derived by the LSP3 with our values. The figure reveals that $\log g$ given by the LSP3 has a linear trend of deviation from our estimated values. The result is consistent with that of Ren et al. (2016), who examined the LSP3 $\log g$ with asteroseismic values from Huber et al. (2014). To better characterize the bias in the LSP3 $\log g$, we display the histogram distribution of $\log\ g$ differences in the right panel in Figure 6. The figure demonstrates that the LSP3 $\log g$ is generally higher than our seismic values by about 0.1 dex, with a calculated standard deviation of 0.16 dex.

We compare the $T_{\rm eff}$–$\log g$ diagram of the LSP3 and our work in Figure 7. The figure indicates that our work yields a sparser distribution, and that a considerable fraction of stars are located in the sub-giant branch. Based on the definition of MSTO stars in Xiang et al. (2015b), our

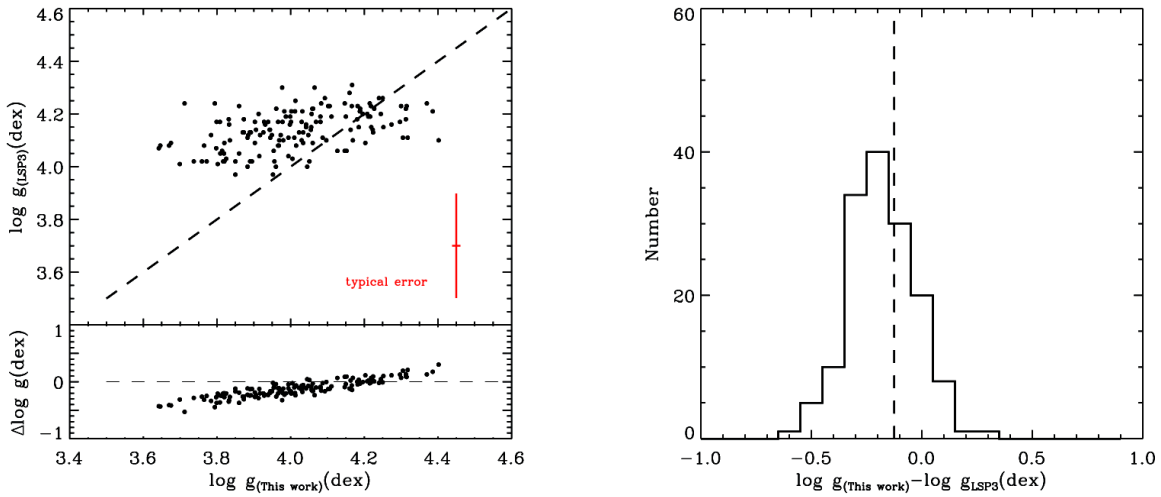

Fig. 6 Comparison of $\log g$, which is derived from LSP3, with our work. *Left panel*: comparison of $\log g$ between LSP3 and our work; the *dashed line* shows the line of equality. *Right panel*: distribution of difference in $\log g$ between LSP3 (LSP3) and this work. The *dashed line* shows the median value of the distribution.

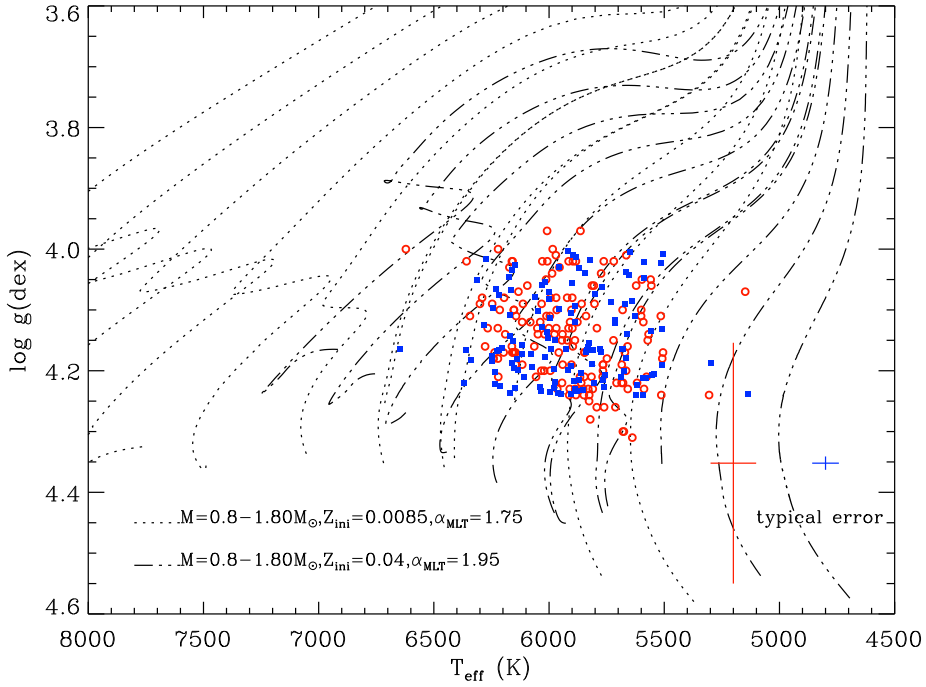

Fig. 7 The location of 150 MSTO candidates with parameters from this work (*blue filled squares*) or the LSP3 (*red open circles*). Typical error bars are presented in the *bottom-right corner* of the figure. *Black dotted lines* and *dash-dotted lines* are evolution tracks for $M = 0.8 - 1.5\ M_{\odot}$ and $Z = 0.0085 - 0.04$ respectively.

revised atmospheric parameters indicate that only 79 of the 150 star candidates are MSTO stars, while the other 71 are contaminations from either main sequence or sub-giant stars. The stellar ages for those 71 contamination stars are marked with red circles in Figure 5. Considering the 29 stars falling outside of our model grids, among which four metal-poor ones may be MSTO stars and the other 25 stars are certainly RGB stars, there are 46% (83/179) stars in total which are MSTO stars, while the others are contaminations from either main sequence or sub-giant stars. However, also considering that the number of stars in our sample is still small, and that the as-

teroseismic samples from literature are probably biased to sub-giant stars because they are brighter and also have relatively larger oscillation amplitudes which are easier to detect, our results have probably overestimated the contamination rate.

5 SUMMARY

Combining atmospheric parameters derived with the LSP3 from LAMOST spectra, and seismic characteristics derived from *Kepler* photometry, we have determined the stellar parameters for 150 MSTO star candidates selected from the MSTO star sample by constructing stellar evolution models. Typical uncertainties in their parameters are $0.04\,M_{\odot}$, $0.03\,L_{\odot}$ and $0.03\,R_{\odot}$ for M, L and R, respectively, $0.4\,\mathrm{Gyr}$ for young stars and $1.3\,\mathrm{Gyr}$ for old stars, as well as $60\,\mathrm{K}$, $0.009\,\mathrm{dex}$ and $0.1\,\mathrm{dex}$ for $T_{\rm eff}$, $\log g$ and [Fe/H], respectively.

In addition, we compare the derived $\log g$, radius and mass with those of Huber et al. (2014), and find that the $\log g$ and radius are very consistent with each other, but the mass shows moderate differences due to different effective temperatures adopted. We also compare our age estimates with those of Xiang et al. (2015b) and find a mean difference of $0.53\,\mathrm{Gyr}$ (7%) and a dispersion of 2.71 Gyr (28%). Moreover, we also re-select MSTO stars based on the criteria of Xiang et al. (2015b) utilizing our newly derived atmospheric parameters and find that about half of the MSTO stars identified with the LSP3 atmospheric parameters are actually main sequence or sub-giant stars, and the stellar ages for those contamination stars are systematically overestimated. The contamination is especially dramatic for the oldest stars in the MSTO star sample. However, the number of stars in our sample is still small, and they are probably biased to subgiant stars, so that our sample may not be representative enough to give a full clarification of the contamination rate of the MSTO star sample. As the LAMOST survey progresses, we plan to obtain a larger sample to deduce more conclusive results in our next work.

Acknowledgements The Guoshoujing Telescope (the Large Sky Area Multi-Object Fiber Spectroscopic Telescope, LAMOST) is a National Major Scientific Project built by the Chinese Academy of Sciences. Funding for the project has been provided by the National Development and Reform Commission. LAMOST is operated and managed by National Astronomical Observatories, Chinese Academy of Sciences. This work is supported by grants 11273007 and 10933002 from the National Natural Science Foundation of China, the Joint Research Fund in Astronomy (U1631236) under cooperative agreement between the National Natural Science Foundation of China (NSFC) and Chinese Academy of Sciences (CAS), the Fundamental Research Funds for the Central Universities and Youth Scholars Program of Beijing Normal University.

References

Appourchaux, T., Chaplin, W. J., García, R. A., et al. 2012, A&A, 543, A54
Bahcall, J. N., Pinsonneault, M. H., & Wasserburg, G. J. 1995, Reviews of Modern Physics, 67, 781
Basu, S., Chaplin, W. J., & Elsworth, Y. 2010, ApJ, 710, 1596
Bedding, T. R., & Kjeldsen, H. 2003, PASA, 20, 203
Bi, S.-L., Basu, S., & Li, L.-H. 2008, ApJ, 673, 1093
Böhm-Vitense, E. 1958, ZAp, 46, 108
Chaplin, W. J., Houdek, G., Appourchaux, T., et al. 2008, A&A, 485, 813
Chaplin, W. J., Kjeldsen, H., Christensen-Dalsgaard, J., et al. 2011, Science, 332, 213
Chaplin, W. J., Basu, S., Huber, D., et al. 2014, ApJS, 210, 1
Christensen-Dalsgaard, J. 1993, in Astronomical Society of the Pacific Conference Series, 42, GONG 1992. Seismic Investigation of the Sun and Stars, ed. T. M. Brown, 347
Cui, X.-Q., Zhao, Y.-H., Chu, Y.-Q., et al. 2012, RAA (Research in Astronomy and Astrophysics), 12, 1197
De Cat, P., Fu, J. N., Ren, A. B., et al. 2015, ApJS, 220, 19
Demarque, P., Guenther, D. B., Li, L. H., Mazumdar, A., & Straka, C. W. 2008, Ap&SS, 316, 31
Demarque, P., Woo, J.-H., Kim, Y.-C., & Yi, S. K. 2004, ApJS, 155, 667
Deng, L.-C., Newberg, H. J., Liu, C., et al. 2012, RAA (Research in Astronomy and Astrophysics), 12, 735
Dotter, A., Chaboyer, B., Jevremović, D., et al. 2008, ApJS, 178, 89
Ferguson, J. W., Alexander, D. R., Allard, F., et al. 2005, ApJ, 623, 585
Gilliland, R. L., Jenkins, J. M., Borucki, W. J., et al. 2010, ApJ, 713, L160
Goudfrooij, P., Puzia, T. H., Kozhurina-Platais, V., & Chandar, R. 2009, AJ, 137, 4988
Grevesse, N., & Sauval, A. J. 1998, Space Sci. Rev., 85, 161
Hekker, S., Elsworth, Y., De Ridder, J., et al. 2011, A&A, 525, A131
Hekker, S., Elsworth, Y., Mosser, B., et al. 2013, A&A, 556, A59
Huang, Y., Liu, X.-W., Yuan, H.-B., et al. 2015, MNRAS, 454, 2863

Huber, D., Chaplin, W. J., Christensen-Dalsgaard, J., et al. 2013, ApJ, 767, 127
Huber, D., Silva Aguirre, V., Matthews, J. M., et al. 2014, ApJS, 211, 2
Iglesias, C. A., & Rogers, F. J. 1996, ApJ, 464, 943
Kallinger, T., Mosser, B., Hekker, S., et al. 2010, A&A, 522, A1
Kjeldsen, H., & Bedding, T. R. 1995, A&A, 293, 87
Liu, X.-W., Yuan, H.-B., Huo, Z.-Y., et al. 2014, in IAU Symposium, 298, Setting the Scene for Gaia and LAMOST, eds. S. Feltzing, G. Zhao, N. A. Walton, & P. Whitelock, 310
Luo, A.-L., Zhao, Y.-H., Zhao, G., et al. 2015, RAA (Research in Astronomy and Astrophysics), 15, 1095
Mackey, A. D., Broby Nielsen, P., Ferguson, A. M. N., & Richardson, J. C. 2008, ApJ, 681, L17
Majewski, S. R., Wilson, J. C., Hearty, F., Schiavon, R. R., & Skrutskie, M. F. 2010, in IAU Symposium, 265, Chemical Abundances in the Universe: Connecting First Stars to Planets, eds. K. Cunha, M. Spite, & B. Barbuy, 480
Mosser, B., Elsworth, Y., Hekker, S., et al. 2012, A&A, 537, A30
Pinsonneault, M. H., Kawaler, S. D., & Demarque, P. 1990, ApJS, 74, 501
Pinsonneault, M. H., Deliyannis, C. P., & Demarque, P. 1992, ApJS, 78, 179
Ren, J.-J., Liu, X.-W., Xiang, M.-S., et al. 2016, RAA (Research in Astronomy and Astrophysics), 16, 45
Rogers, F. J., & Nayfonov, A. 2002, ApJ, 576, 1064
Steinmetz, M., Zwitter, T., Siebert, A., et al. 2006, AJ, 132, 1645
Stello, D., Huber, D., Bedding, T. R., et al. 2013, ApJ, 765, L41
Thoul, A. A., Bahcall, J. N., & Loeb, A. 1994, ApJ, 421, 828
Tian, Z., Bi, S., Bedding, T. R., & Yang, W. 2015, A&A, 580, A44
Wang, L., Wang, W., Wu, Y., et al. 2016, AJ, 152, 6
Wu, Y., Du, B., Luo, A., Zhao, Y., & Yuan, H. 2014, in IAU Symposium, 306, Statistical Challenges in 21st Century Cosmology, eds. A. Heavens, J.-L. Starck, & A. Krone-Martins, 340
Xiang, M. S., Liu, X. W., Yuan, H. B., et al. 2015a, RAA (Research in Astronomy and Astrophysics), 15, 1209
Xiang, M. S., Liu, X. W., Yuan, H. B., et al. 2015b, MNRAS, 448, 822
Yang, W., Bi, S., Meng, X., & Liu, Z. 2013, ApJ, 776, 112
Yang, W., & Meng, X. 2010, New Astron., 15, 367
Yanny, B., Newberg, H. J., Johnson, J. A., et al. 2009, ApJ, 700, 1282
Zhao, G., Zhao, Y.-H., Chu, Y.-Q., Jing, Y.-P., & Deng, L.-C. 2012, RAA (Research in Astronomy and Astrophysics), 12, 723